Molecular Neurobiology (2019) 56:1366–1390
https://doi.org/10.1007/s12035-018-1114-9

Multifaceted Regulation of ALDH1A1 by Cdk5 in Alzheimer's Disease Pathogenesis

Kumar Nikhil[1] · Keith Viccaro[1] · Kavita Shah[1]

Received: 22 February 2018 / Accepted: 9 May 2018 / Published online: 8 June 2018

Abstract

This study revealed multifaceted regulation of ALDH1A1 by Cdk5 in Alzheimer's disease (AD) pathogenesis. ALDH1A1 is a multifunctional enzyme with dehydrogenase, esterase, and anti-oxidant activities. ALDH1A1 is also a major regulator of retinoic acid (RA) signaling, which is critical for normal brain homeostasis. We identified ALDH1A1 as both physiological and pathological target of Cdk5. First, under neurotoxic conditions, Cdk5-induced oxidative stress upregulates *ALDH1A1* transcription. Second, Cdk5 increases ALDH1A1 levels by preventing its ubiquitylation via direct phosphorylation. Third, ALDH1A1 phosphorylation increases its dehydrogenase activity by altering its tetrameric state to a highly active monomeric state. Fourth, persistent oxidative stress triggered by deregulated Cdk5 inactivates ALDH1A1. Thus, initially, the good Cdk5 attempts to mitigate ensuing oxidative stress by upregulating ALDH1A1 via phosphorylation and paradoxically by increasing oxidative stress. Later, sustained oxidative stress generated by Cdk5 inhibits ALDH1A1 activity, leading to neurotoxicity. ALDH1A1 upregulation is highly neuroprotective. In human AD tissues, ALDH1A1 levels increase with disease severity. However, ALDH1A1 activity was highest at mild and moderate stages, but declines significantly at severe stage. These findings confirm that during the initial stages, neurons attempt to upregulate and activate ALDH1A1 to protect from accruing oxidative stress-induced damage; however, persistently deleterious conditions inactivate ALDH1A1, further contributing to neurotoxicity. This study thus revealed two faces of Cdk5, good and bad in neuronal function and survival, with a single substrate, ALDH1A1. The bad Cdk5 prevails in the end, overriding the good Cdk5 act, suggesting that Cdk5 is an effective therapeutic target for AD.

Keywords Cdk5 · ALDH1A1 · Alzheimer's disease · Neurodegeneration · Chemical genetic · Neuroprotection

Abbreviations

Cdk5	Cyclin-dependent kinase-5
AD	Alzheimer's disease
ALDH1A1	Aldehyde dehydrogenase A1 isoform

Introduction

Alzheimer's disease (AD) is a progressive neurodegenerative condition which affects over 25 million people worldwide [1]. Oxidative stress is believed to be one of the earliest events in AD, which occur prior to the onset of significant plaque accumulation. Recent evidence further support a pivotal role of dysfunctional retinoic acid (RA) signaling in the formation of neurotoxic β-amyloid (Aβ) and neurofibrillary tangles (NFT), the two hallmarks of AD [2–5]. RA agonists are strikingly effective in restoring synaptic functions and clearing Aβ, which underscores the clinical significance of this pathway for developing effective therapies. However, an incomplete understanding of the underlying mechanisms has hindered the characterization of early detection biomarkers and the development of target-based therapies.

We focused on cyclin-dependent kinase-5 (Cdk5), which is deregulated in AD brains and contributes significantly to the formation of Aβ plaques and NFT, and promotes neurodegeneration [6–11]. Cdk5 is highly active in post-mitotic neurons. During embryogenesis, Cdk5 is essential for brain development [12]. Postnatally, Cdk5 is critical for higher cognitive functions such as synaptic plasticity, learning and memory formation, and drug addiction [13, 14]. Reduction or loss of

Electronic supplementary material The online version of this article (https://doi.org/10.1007/s12035-018-1114-9) contains supplementary material, which is available to authorized users.

✉ Kavita Shah
shah23@purdue.edu

[1] Department of Chemistry and Purdue University Center for Cancer Research, Purdue University, 560 Oval Drive West, Lafayette, IN 47907, USA

Cdk5 activity is linked with mental retardation, schizophrenia, epilepsy, and attention-deficit/hyperactivity disorder [15–18]. Similarly, Cdk5 is hyperactivated in many neurological disorders including AD, Parkinson's disease (PD), ischemic stroke, and amyotrophic lateral sclerosis (ALS) and is highly neurotoxic [19, 20].

In AD, neurotoxic signals such as excitotoxicity, Aβ, ischemia, and oxidative stress increase intracellular calcium levels in neurons, resulting in calpain activation, which cleaves Cdk5 activator p35 into p25 and p10. Cdk5-p25 complex is constitutively activated and mislocalized, resulting in the phosphorylation of many non-physiological targets, culminating into neuronal death [21, 22]. A pivotal role of the Cdk5-p25 complex in promoting AD pathogenesis was recently shown in a mouse model, where specific inhibition of aberrant Cdk5 activity using a peptide inhibitor attenuated NFT formation and restored synaptic and cognitive functions [23].

We recently identified aldehyde dehydrogenase A1 isoform (ALDH1A1) as a direct target of Cdk5 in mouse brain lysates. ALDH1A1 is a multifunctional enzyme with dehydrogenase, esterase, and anti-oxidant activities [24, 25]. *ALDH1A1* is widely expressed in the brain; however, its exact role in AD pathogenesis remains unclear [26]. ALDH1A1 overexpression is neuroprotective under neurotoxic conditions in cells [27–29]; however, whether neurotoxicity impacts endogenous ALDH1A1 levels and activity remains unknown. The temporal correlation between ALDH1A1 protein levels and activity with AD disease progression is yet to be analyzed. Notably, ALDH1A1 catalyzes the conversion of retinal to retinoic acid (RA) and thus is a major regulator of RA signaling, which is essential for normal brain homeostasis [2–5]. We unraveled a molecular mechanism by which ALDH1A1 levels and activity are regulated under neurotoxic conditions in HT22 (mouse hippocampal cell line) and primary cortical neurons. We also uncovered the consequences of ALDH1A1 regulation on ensuing oxidative stress. The clinical significance of our finding was confirmed in human clinical specimens, which revealed the correlation between ALDH1A1 activity and levels with disease progression.

Results

ALDH1A1 Is a Direct Substrate of Cdk5

We have developed a chemical genetic approach to identify the direct substrates of any kinase of interest on a proteome-wide scale [30–37]. This approach involves an engineered kinase (e.g., Cdk5-as1), which uses a radioactive orthogonal ATP analog (e.g., N-6-phenethyl-ATP), and specifically transfers the radioactive tag (^{32}P) to its substrates. Using this methodology, we have identified several direct substrates of Cdk5 including GM130, peroxiredoxin 1, peroxiredoxin 2, lamin A, lamin B, Cdc25A, Cdc25B, Cdc25C, FOXO3a, and Mcl-1 [38–43]. In this study, we focused on Cdk5-mediated regulation of ALDH1A1 signaling. As proteomics screen can often yield false positives, we examined whether Cdk5 directly phosphorylates ALDH1A1 using an in vitro kinase assay. Cdk5 directly phosphorylates ALDH1A1, confirming that it is a direct substrate of Cdk5 (Fig. 1a).

Cdk5 and ALDH1A1 Associate Directly in Glutamate-Treated HT22 Cells

To uncover the significance of ALDH1A1 phosphorylation by Cdk5, we examined their association with each other in HT22 cells under normal and neurotoxic conditions. Glutamate was chosen as the neurotoxic signal. Glutamate excitotoxicity is a major contributor to AD pathogenesis. We isolated Cdk5 immune complex, which revealed no association of Cdk5 with

Fig. 1 ALDH1A1 is a disease-specific target of Cdk5. **a** ALDH1A1 is a direct substrate of Cdk5. Cdk5-p25 complex was subjected to kinase assay with either [^{32}P]ATP alone (lane 2) or with 6× His-ALDH1A1 and [^{32}P]ATP (lane 3) for 15 min. Lane 1 shows ALDH1A1 incubated with [^{32}P]ATP. **b** Cdk5 and ALDH1A1 associate under neurotoxic conditions in HT22 cells. Cdk5 was immunoprecipitated from either control or glutamate-treated HT22 cells (for 0–6 h), and the association of Cdk5 and ALDH1A1 was analyzed (*top panel*). *Lower panel* shows Cdk5 input from total cell lysate. Each experiment was repeated at least three independent times. **c** Cdk5 and ALDH1A1 association under normal and neurotoxic conditions in HT22 cells. ALDH1A1 was immunoprecipitated from either control or glutamate-treated HT22 cells (for 0–6 h), and the association of ALDH1A1 and Cdk5 analyzed. *Lower panel* shows ALDH1A1 levels from total cell lysate. **d** Cdk5 binds ALDH1A1 directly. ALDH1A1 and Cdk5 association was analyzed using recombinant Cdk5 and ALDH1A1 in an in vitro pull-down assay. 6× His-Cdk5 on beads was incubated with ALDH1A1 and their binding analyzed. **e** Cdk5 and ALDH1A1 bind directly. ALDH1A1 on beads was incubated with recombinant Cdk5 and their binding analyzed in an in vitro pull-down assay. **f** Glutamate stimulates the association of p35/p25 with ALDH1A1. p35/p25 were immunoprecipitated from either control or glutamate-treated HT22 cells (for 0–6 h), and the association of p35/p25 with ALDH1A1 analyzed. Each experiment was repeated at least three independent times. **g** Glutamate stimulates association of p35/p25 and ALDH1A1. ALDH1A1 was immunoprecipitated from either control or glutamate-treated HT22 cells (for 0–6 h), and the association of ALDH1A1 and p35/p25 was analyzed. Each experiment was repeated at least three independent times. **h** ALDH1A1 does not bind with p35 or p25 directly. ALDH1A1 and p35 or p25 association was analyzed using recombinant p35, p25, and ALDH1A1 in an in vitro pull-down assay. Recombinant ALDH1A1 on beads was incubated with 6× His-p35 or 6× His-p25 and binding analyzed. **i** Cdk5 associates with p35/p25 upon glutamate stimulation. p35/p25 were immunoprecipitated from either control or glutamate-treated HT22 cells (for 0–6 h), and the association of p35/p25 with Cdk5 analyzed. Each experiment was repeated at least three independent times. **j** Cdk5 associates with p35 and p25 upon glutamate stimulation. **k** Cdk5 activity increases upon glutamate treatment in HT22 cells. Cdk5 kinase assay was performed as described in the "Materials and Methods" section. Each experiment was repeated at least three independent times. *$p < 0.05$, compared with untreated HT22 cells

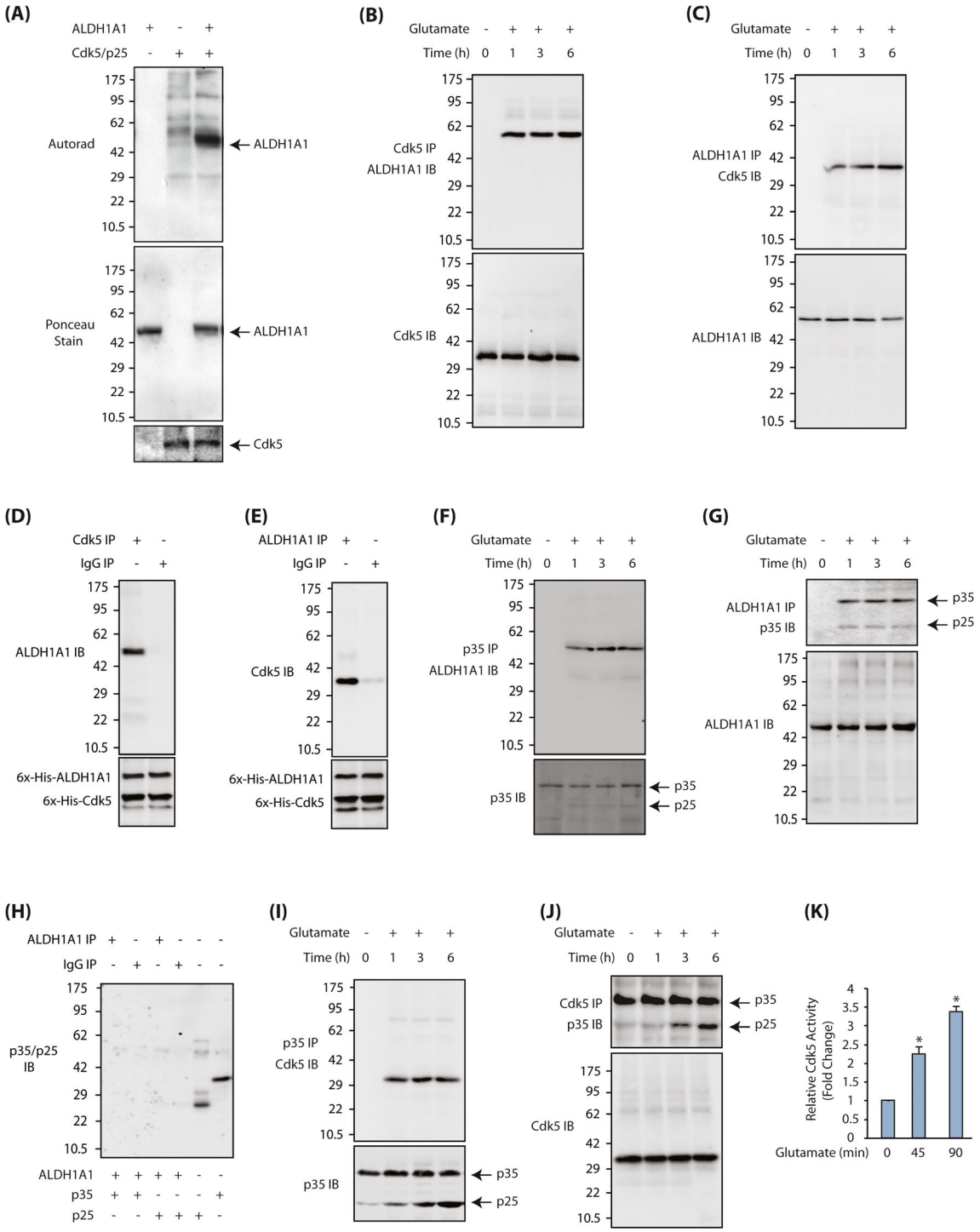

ALDH1A1 in control cells (Fig. 1b, lane 1). However, upon glutamate treatment, a time-dependent increase in the association between Cdk5 and ALDH1A1 was observed. These results were confirmed by reciprocal immunoprecipitation, where ALDH1A1 immune complexes were isolated, which also revealed increased association of Cdk5 and ALDH1A1 upon glutamate treatment (Fig. 1c).

To examine whether their association was direct or indirect, we conducted in an in vitro pull-down assay using recombinant Cdk5 and ALDH1A1. IgG was used as a negative control. Cdk5 on beads was incubated with recombinant ALDH1A1, which pulled down ALDH1A1 (Fig. 1d). Similarly, ALDH1A1 immune complex pulled down Cdk5, confirming a direct association between these proteins (Fig. 1e).

This finding prompted us to investigate whether ALDH1A1 binds to Cdk5 activators, p35, or p25 in HT22 cells. The p35/p25 immune complexes were isolated from untreated and glutamate-treated HT22 cells, and their potential binding to ALDH1A1 analyzed. Glutamate treatment triggered the formation of p25 as expected (Fig. 1f). As observed for Cdk5 immune complex, ALDH1A1 was only present in glutamate-treated cells, suggesting that ALDH1A1 associates with p35/p25 specifically under neurotoxic conditions (Fig. 1f). Similarly, when ALDH1A1 was isolated, p35/p25 were present only in glutamate-exposed cells (Fig. 1g). These results confirm that Cdk5 and p35/p25 associate with ALDH1A1 under neurotoxic conditions.

We next investigated potential binding of p35 and p25 to ALDH1A1 independent of Cdk5 in an in vitro binding assay using purified recombinant ALDH1A1, p35 and p25. IgG was used as a negative control. Recombinant ALDH1A1 on beads was either incubated with 6× His-p35 or 6× His-p25. ALDH1A1 immune complex showed no binding with either p35 or p25, suggesting that the presence of ALDH1A1 in p35/p25 complex is due to its binding with Cdk5 (Fig. 1h).

To confirm this finding, we analyzed Cdk5 levels in the p35/p25 immune complex, which associated with p35 and p25 only in glutamate-treated cells (Fig. 1i). In a reciprocal experiment, Cdk5 immune complex was isolated from control and glutamate-treated cells and p35 and p25 levels analyzed. As predicted, p35 and p25 were present predominantly in the glutamate-exposed cells (Fig. 1j). Since p25 binding increases Cdk5 activity, we also measured Cdk5 activity in these cells. Cdk5 activity increases > 2-fold after glutamate treatment (Fig. 1k). These results reveal that ALDH1A1 directly binds to Cdk5 upon neurotoxic stimulation, suggesting that ALDH1A1 may be a disease-specific target of Cdk5.

Cdk5 Regulates the Subcellular Localization of ALDH1A1 in HT22 Cells

Direct association of Cdk5 and ALDH1A1 in glutamate-exposed HT22 cells prompted us to investigate their subcellular localization in HT22 cells. In untreated cells, Cdk5 and ALDH1A1 were cytoplasmic (Fig. 2a). Glutamate exposure triggered an increased nuclear translocation of both Cdk5 and ALDH1A1 (Fig. 2a, b). Cdk5 inhibition using roscovitine retained both ALDH1A1 and Cdk5 in the cytoplasm, suggesting that they not only co-localize but that Cdk5 also regulates the subcellular localization of ALDH1A1 (Fig. 2a, b). We also conducted cytosolic and nuclear fractionation of control and treated cells, which too revealed increased nuclear translocation of Cdk5 and ALDH1A1 upon glutamate stimulation, which was Cdk5-dependent (Fig. 2c).

Cdk5 Knockdown Inhibits Nuclear Translocation of ALDH1A1

We also knocked down Cdk5, which completely inhibited nuclear translocation of ALDH1A1 triggered by glutamate (Fig. 2d, e). Nuclear and cytoplasmic fractions of control and treated cells further confirmed these results (Fig. 2f). Notably, increased levels of lamin A were observed in the cytosolic fraction of glutamate-treated cells (Fig. 2c), compared to Cdk5-inhibited (Fig. 2c) or Cdk5-depleted cells (Fig. 2f). This finding is consistent with our previous report that showed rapid dispersion of nuclear lamina in glutamate-treated cells triggered by Cdk5-mediated phosphorylation of lamin A and lamin B1 [40].

Cdk5 Phosphorylates ALDH1A1 at S75 and S274

Cdk5 is a proline-directed kinase which preferentially phosphorylates SP and TP sites with adjacent basic residues. Based on this preference, we generated two phospho-resistant mutants of ALDH1A1 (S75A and S274A, human numbering) and subjected them to kinase assays using Cdk5-p25. ALDH1A1 was phosphorylated at both of these sites by Cdk5-p25 (Fig. 3a). However, we consistently observed that S75 was the preferential phosphorylation site, as S75A mutant showed reduced phosphorylation compared to S274 site. The corresponding double mutant (S75A, S274A)-ALDH1A1 (abbreviated as 2A-ALDH1A1) was not phosphorylated by Cdk5-p25, suggesting that these are the only Cdk5 sites on ALDH1A1 (Fig. 3b).

Fig. 2 Cdk5 promotes nuclear localization of ALDH1A1 upon glutamate stimulation. **a** Glutamate stimulates nuclear translocation of Cdk5 and ALDH1A1. HT22 cells were treated with glutamate for 0–12 h with or without roscovitine, followed by immunostaining as described in the "Materials and Methods" section. Representative pictures are shown. Scale bar, 20 μm. **b** Quantification of the subcellular localization of ALDH1A1 in the cell nucleus versus the cytoplasm. The graphs show the mean ± SEM of the relative fluorescence intensity with respect to control cells. $*p < 0.05$ versus nucleus fraction control analyzed by two-way analysis of variance. **c** Subcellular fractionation of ALDH1A1 in glutamate-treated HT22 cells in the absence or presence of roscovitine as described in the "Materials and Methods" section. Alpha-tubulin is the cytoplasmic marker and lamin A is the nuclear marker. *N* nuclear fraction, *C* cytoplasmic fraction. **d** Cdk5 knockdown inhibits nuclear translocation of ALDH1A1. HT22 cells were treated with Cdk5 shRNA for 30 h, followed by glutamate treatment for 1.5–12 h. **e** Quantification of the subcellular localization of ALDH1A1 in the cell nucleus versus the cytoplasm. The graphs show the mean ± SEM of the relative fluorescence intensity with respect to control cells. **f** Cdk5 shRNA-infected HT22 cells were treated with glutamate and fractionated as described in the "Materials and Methods" section. Alpha-tubulin is the cytoplasmic marker and lamin A is the nuclear marker. *N* nuclear fraction, *C* cytoplasmic fraction

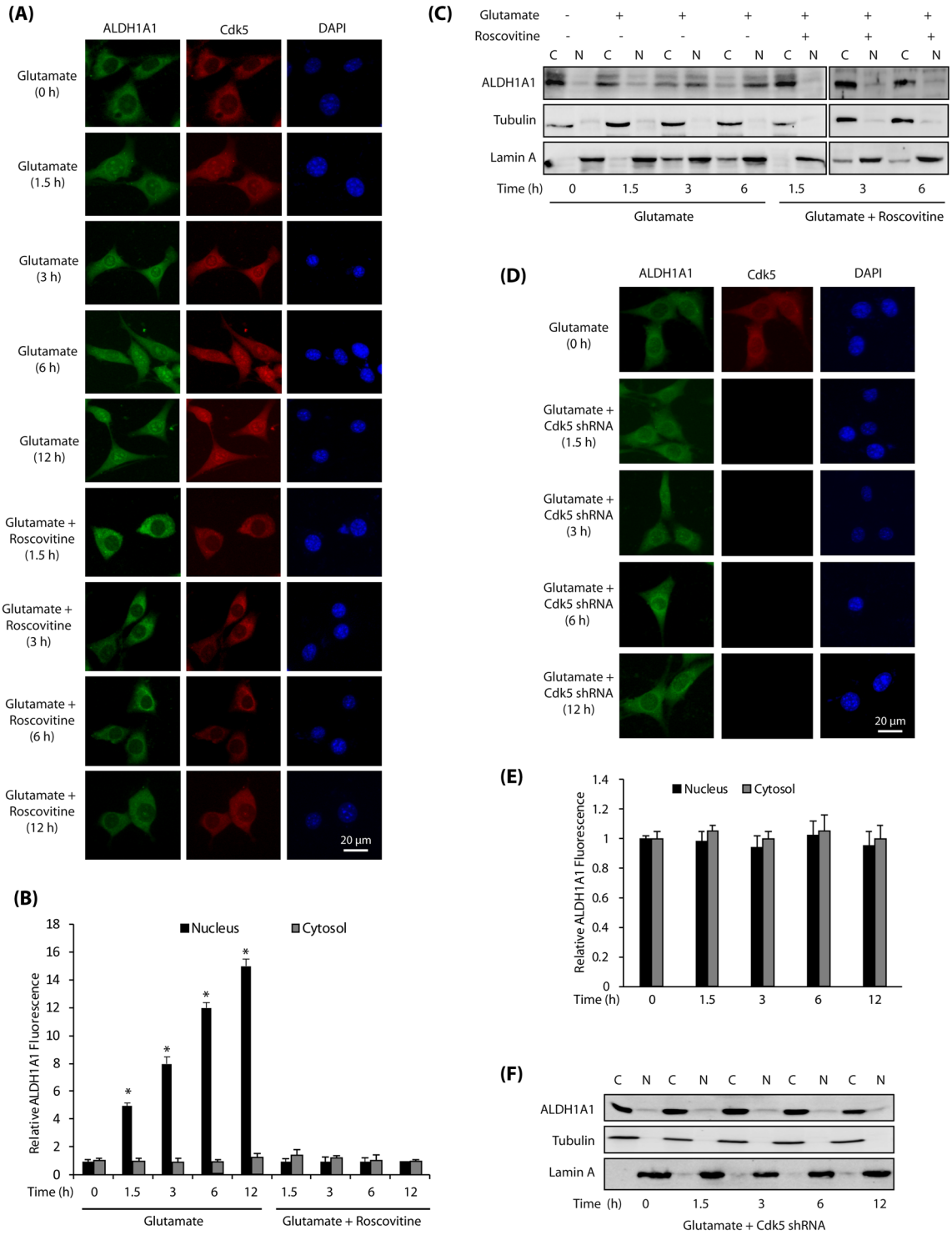

Cdk5-Mediated Nuclear Envelop Dispersion Is Responsible for the Nuclear Translocation of ALDH1A1

To uncover the consequences of Cdk5-mediated phosphorylation of ALDH1A1, we generated wild-type HA-tagged ALDH1A1-expressing and phosphorylation-resistant HA-tagged 2A-ALDH1A1-expressing HT22 cells and exposed them to glutamate for varying periods (0, 1.5, 3, 6, and 12 h). As expected, ALDH1A1-HT22 cells displayed nuclear localization of ectopically expressed ALDH1A1, which was Cdk5 dependent (Fig. 3c, d). Nuclear and cytosolic fractionation further validated that Cdk5 triggers ALDH1A1 migration to the nucleus in glutamate-treated cells (Fig. 3e).

Similarly, Cdk5 knockdown resulted in complete inhibition of ALDH1A1 nuclear translocation in the presence of glutamate (Fig. 3f, g). These findings show that wild-type HA-tagged ALDH1A1 behaves similarly to endogenous ALDH1A1 and shows identical subcellular localization and migration in control and glutamate-treated HT22 cells.

We next exposed phosphorylation-resistant 2A-ALDH1A1-HT22 cells to glutamate for varying periods. Similar to wild-type ALDH1A1-HT22 cells, glutamate treatment triggered robust nuclear localization of Cdk5 (Fig. 4a, b). Interestingly, phosphorylation-dead 2A-ALDH1A1 also migrated to the nucleus following glutamate exposure (analyzed using HA antibody), suggesting that Cdk5-mediated phosphorylation of ALDH1A1 is not responsible for its nuclear translocation (Fig. 4a, c). Cytoplasmic and nuclear fractionation further confirmed this finding (Fig. 4d). These data show that although nuclear translocation of ALDH1A1 depends on Cdk5, it is not due to Cdk5-mediated phosphorylation. Since Cdk5 deregulation leads to nuclear envelop dispersion (Fig. 2c), these data suggest that ALDH1A1 is mislocalized to the nucleus due to nuclear lamina fragmentation.

Cdk5 Increases ALDH1A1 Messenger RNA Levels in Glutamate-Treated HT22 Cells

We next examined the consequences of ALDH1A1 regulation under neurotoxic conditions, and whether it was mediated by Cdk5. HT22 cells were treated with glutamate for either 12 or 24 h, which resulted in moderate increase in its messenger RNA (mRNA) levels (~1.3- and 1.7-fold, respectively, analyzed by semi-quantitative PCR). Cdk5 ablation largely prevented this increase in ALDH1A1 transcription, particularly at 24 h, suggesting that this process is Cdk5-dependent (Supplementary Fig. 2A, B). We also analyzed ALDH1A1 transcript levels in glutamate-treated HT22 cells using real-time qPCR, which further supported that the modest increase in ALDH1A1 transcript levels in neurotoxin-exposed cells is regulated by Cdk5 (Fig. 4e).

Cdk5-Mediated Phosphorylation Increases ALDH1A1 Protein Levels in Glutamate-Treated HT22 Cells

As Cdk5 directly phosphorylates ALDH1A1, we investigated whether it was also regulated post-translationally in HT22 cells. Glutamate treatment for 6 h resulted in > 2-fold increase in ALDH1A1 levels, which increased to ~3-fold at 12 h and remained constant at 24 h (Fig. 4f, g). To determine whether this increase was mediated by Cdk5, ALDH1A1 levels were examined in glutamate-exposed HT22 cells (12 h) with or without Cdk5 shRNA or roscovitine. Glutamate treatment resulted in significant increase in ALDH1A1 levels which was inhibited by Cdk5 inhibition or depletion (Fig. 4h, i).

As the increase in ALDH1A1 protein levels was significantly higher than its mRNA levels, it suggested that ALDH1A1 is also regulated post-translationally. Thus, we exposed ALDH1A1-HT22 and 2A-ALDH1A1-HT22 cells to glutamate for 12 h with or without roscovitine or Cdk5 shRNA. In glutamate-treated ALDH1A1-HT22 cells, ALDH1A1 levels increased in a Cdk5-dependent manner (Supplementary Fig. 2C, D). Both Cdk5 inhibition and knockdown inhibited increase in ALDH1A1 levels, suggesting it to be a Cdk5-dependent process (Fig. 4j, k).

In contrast, 2A-ALDH1A1-HT22 cells exhibited a modest increase in 2A-ALDH1A1 levels compared to ALDH1A1-HT22 cells upon glutamate exposure (Fig. 4l, m). This finding was further supported by Cdk5 knockdown and inhibition, which had little effect on phosphorylation-dead ALDH1A1 levels (Fig. 4n, o). These results demonstrate that Cdk5 increases ALDH1A1 levels in neurotoxin-exposed neuronal cells both at transcriptional level and by direct phosphorylation at S75 and S274 sites.

Cdk5 Activates ALDH1A1 Dehydrogenase Activity Via Phosphorylation

ALDH1A1 has a NAD^+ binding pocket (amino acids 8–135 and 159–270), a catalytic site (271–470), and an oligomerization domain (amino acids 140–158 and 486–495). S75 is present within the NAD^+ binding pocket and S274 is part of the catalytic site, buried deep in the binding pocket (Fig. 5a). The neighboring E269 residue in the active site is crucial for catalysis. We phosphorylated ALDH1A1 (expressed as 6× His-tagged protein in *Escherichia coli*) using Cdk5-p25, which triggered a robust increase in ALDH1A1 activity (Fig. 5b).

Fig. 3 Cdk5 directly phosphorylates ALDH1A1 at S75 and S274. **a** The Cdk5-p25 complex (Cdk5/p25) phosphorylates ALDH1A1 at S75 and S274. Recombinant 6× His-tagged wild-type and ALDH1A1 mutants were subjected to a kinase assay with Cdk5-p25. **b** S75 and S274 are the only Cdk5 sites on ALDH1A1, as the 2A-ALDH1A1 mutant is not phosphorylated by Cdk5. **c** Glutamate stimulates nuclear translocation of Cdk5 and ALDH1A1 in ALDH1A1-HT22 cells. ALDH1A1-HT22 cells were treated with glutamate for 0–12 h with or without roscovitine, followed by immunostaining with anti-HA and Cdk5 antibody. Representative pictures are shown. **d** Quantification of the subcellular localization of ALDH1A1 in the cell nucleus versus the cytoplasm. The graphs show the mean ± SEM of the relative fluorescence intensity with respect to control cells. $*p < 0.05$ versus nucleus fraction control analyzed by two-way analysis of variance. **e** Subcellular fractionation of ALDH1A1 in glutamate-treated ALDH1A1-HT22 cells in the absence or presence of roscovitine. Alpha-tubulin is the cytoplasmic marker and lamin A is the nuclear marker. *N* nuclear fraction, *C* cytoplasmic fraction. **f** Cdk5 knockdown inhibits nuclear translocation of ALDH1A1. Cdk5-shRNA-infected ALDH1A1-HT22 cells were treated with glutamate. Representative pictures are shown. **g** Quantification of the subcellular localization of ALDH1A1 in the cell nucleus versus the cytoplasm. The graphs show the mean ± SEM of the relative fluorescence intensity with respect to control cells

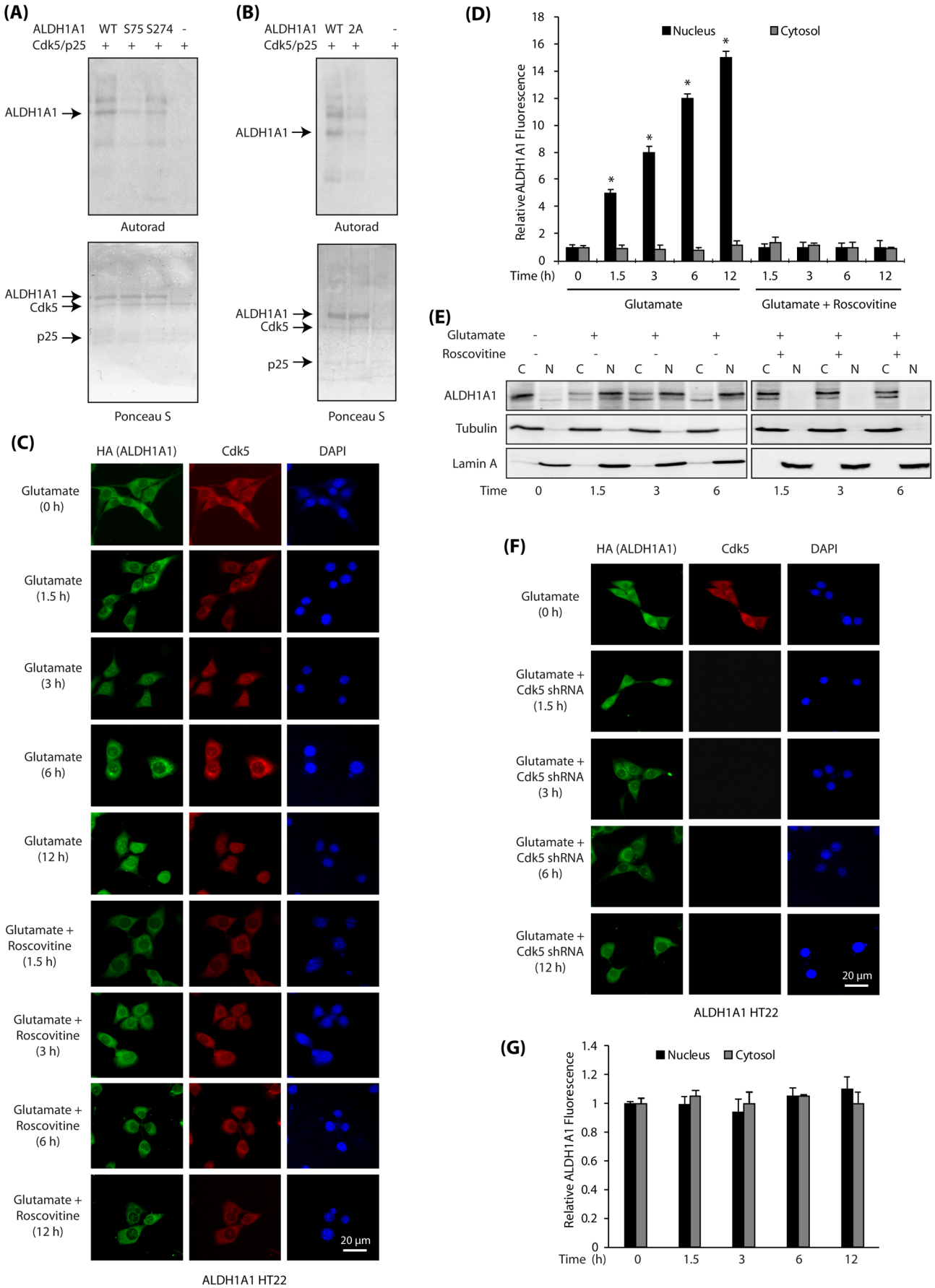
(A)
ALDH1A1 WT S75 S274 -
Cdk5/p25 + + + +
ALDH1A1
Autorad
ALDH1A1
Cdk5
p25
Ponceau S
(B)
ALDH1A1 WT 2A -
Cdk5/p25 + + +
ALDH1A1
Autorad
ALDH1A1
Cdk5
p25
Ponceau S
(C)
HA (ALDH1A1)
Cdk5
DAPI
Glutamate (0 h)
Glutamate (1.5 h)
Glutamate (3 h)
Glutamate (6 h)
Glutamate (12 h)
Glutamate + Roscovitine (1.5 h)
Glutamate + Roscovitine (3 h)
Glutamate + Roscovitine (6 h)
Glutamate + Roscovitine (12 h)
20 μm
ALDH1A1 HT22
(D)
Nucleus
Cytosol
Relative ALDH1A1 Fluorescence
Time (h) 0 1.5 3 6 12 1.5 3 6 12
Glutamate
Glutamate + Roscovitine
(E)
Glutamate
Roscovitine
C N C N C N C N C N C N C N
ALDH1A1
Tubulin
Lamin A
Time 0 1.5 3 6 1.5 3 6
(F)
HA (ALDH1A1)
Cdk5
DAPI
Glutamate (0 h)
Glutamate + Cdk5 shRNA (1.5 h)
Glutamate + Cdk5 shRNA (3 h)
Glutamate + Cdk5 shRNA (6 h)
Glutamate + Cdk5 shRNA (12 h)
20 μm
ALDH1A1 HT22
(G)
Nucleus
Cytosol
Relative ALDH1A1 Fluorescence
Time (h) 0 1.5 3 6 12

Supplementary Figure 3A shows relative ALDH1A1 activity after 150 min. This increase was diminished upon treatment with calf-intestinal alkaline phosphatase (Fig. 5c). Cdk5-mediated increase in ALDH1A1 activity suggested that phosphorylation-dead ALDH1A1 mutant may possess low intrinsic activity. However, the complete lack of activity observed in 2A-ALDH1A1 mutant suggested that mutations at S75 and S274 likely perturb either NAD^+ binding and/or impair the catalytic activity of ALDH1A1, rendering it inactive (Fig. 5d and Supplementary Fig. 3B).

Cdk5-Mediated Phosphorylation of ALDH1A1 Regulates Its Oligomeric States

ALDH1A1 can exist in monomeric, dimeric, or tetrameric forms. At high concentrations, it predominantly exists as tetramer, similar to most oligomeric proteins. We observed little dimer at all concentrations, suggesting that the tetramer and the monomer are most abundant forms of ALDH1A1. We recently reported that aurora kinase A (AURKA)-mediated phosphorylation of ALDH1A1 triggers the formation of monomers, which possess higher intrinsic activity [36]. Therefore, we hypothesized that Cdk5-mediated phosphorylation of ALDH1A1 may too alter its oligomeric state.

As the phosphorylation advanced, ALDH1A1 oligomeric distribution significantly shifted towards the monomeric form (Fig. 5e). The simultaneous decrease in tetramer concentration served as an internal control to confirm its dissociation upon phosphorylation. Figure 5f displays average relative changes in tetramer and monomer abundance upon Cdk5-mediated phosphorylation. Figure 5g shows average ratio of normalized monomer to tetramer as a function of time derived from three independent experiments.

We conducted a similar kinetic analysis and measured the dehydrogenase activity of ALDH1A1 using a native in-gel activity assay to determine which oligomeric species had the highest activity with and without phosphorylation. Upon phosphorylation, the monomeric species exhibited the highest activity (> 3-fold increase), whereas the tetramer showed little to no change (Fig. 5h, i). Figure 5j shows quantification of oligomer-specific ALDH1A1 activities from three independent experiments.

We next sought the oligomeric species that was most phosphorylated to examine a potential correlation between phosphorylation and activity. As predicted, the monomeric population which was formed was highly phosphorylated (Fig. 5k–m). These data suggest that ALDH1A1 phosphorylation triggers the dissociation of the tetramer into monomer. Furthermore, the most phosphorylated monomer exhibits the highest enzymatic activity among all of the oligomeric species.

Cdk5 Plays a Neuroprotective Role by Upregulating ALDH1A1 in Glutamate-Exposed Cells

Cdk5 deregulation is known to trigger several neurodegenerative pathways. Since ALDH1A1 was both activated and upregulated in a Cdk5-dependent manner, we examined whether modulation of ALDH1A1 levels conferred neuroprotection or neurotoxicity in control and glutamate-treated cells. We exposed HT22 cells to glutamate for 24 h, which resulted in > 50% loss in cell viability. Cdk5 depletion largely protected these cells (Fig. 6a). In contrast, Cdk5 inhibition using roscovitine was partially neuroprotective, which was consistent with our

Fig. 4 ALDH1A1 translocation to the nucleus is phosphorylation-independent. **a** 2A-ALDH1A1-HT22 cells were treated with glutamate for 0–12 h, followed by immunostaining with anti-HA antibody. Representative pictures are shown. **b** Quantification of the subcellular localization of Cdk5 in the cell nucleus versus the cytoplasm. The graphs show the mean ± SEM of the relative fluorescence intensity with respect to control cells. $^*p < 0.05$ versus nucleus fraction control analyzed by two-way analysis of variance. **c** Quantification of the subcellular localization of ALDH1A1 in the cell nucleus versus the cytoplasm. The graphs show the mean ± SEM of the relative fluorescence intensity with respect to control cells. $^*p < 0.05$ versus nucleus fraction control analyzed by two-way analysis of variance. **d** Subcellular fractionation of 2A-ALDH1A1 in glutamate-treated 2A-ALDH1A1-HT22 cells. 2A-ALDH1A1 was visualized using anti-HA antibody. Alpha-tubulin is the cytoplasmic marker and lamin A is the nuclear marker. *N* nuclear fraction, *C* cytoplasmic fraction. **e** HT22 cells were treated with glutamate and Cdk5 shRNA and total mRNA levels of ALDH1A1 were detected by real-time qPCR. Expression levels are normalized to the expression of actin. Results are mean ± SEM of three independent experiments. $^*p < 0.05$, compared with untreated HT22 cells. $^{\#}p < 0.05$, compared with only glutamate-treated HT22 cells. **f** HT22 cells were treated with glutamate for 0–24 h and the total levels of ALDH1A1 analyzed. **g** Average relative ratios of ALDH1A1 band intensities to alpha-tubulin band intensities upon glutamate treatment as obtained from three independent experiments. $^*p < 0.05$, compared with untreated HT22 cells. **h** HT22 cells were treated with glutamate for 12 h, in the presence and absence of roscovitine or Cdk5 shRNA, and then, the total levels of ALDH1A1 were analyzed. **i** ALDH1A1 protein levels in HT22 cells in response to glutamate treatment with or without roscovitine and Cdk5 shRNA. Graphical results are mean ± SEM of three independent experiments. $^*p < 0.05$, compared with untreated HT22 cells. $^{\#}p < 0.05$, compared with only glutamate-treated HT22 cells. **j** ALDH1A1-HT22 cells were treated similarly as in h and the ALDH1A1 levels analyzed. **k** ALDH1A1 protein levels in ALDH1A1-HT22 cells in response to glutamate treatment with or without roscovitine and Cdk5 shRNA. Graphical results are mean ± SEM of three independent experiments. $^*p < 0.05$, compared with untreated ALDH1A1-HT22 cells, and $p < 0.05$, compared with only glutamate-treated HT22 cells. **l** 2A-ALDH1A1-HT22 cells were treated similarly as in f and total levels of ALDH1A1 analyzed. **m** Average relative ratios of HA (ALDH1A1) band intensities to alpha-tubulin band intensities upon glutamate treatment as obtained from three independent experiments. $^*p < 0.05$, compared with untreated 2A-ALDH1A1-HT22 cells. **n** 2A-ALDH1A1-HT22 cells were treated similarly as in h and the ALDH1A1 levels analyzed. **o** ALDH1A1 protein levels in HT22 cells in response to glutamate treatment with or without roscovitine and Cdk5 shRNA. Graphical results are mean ± SEM of three independent experiments. $^*p < 0.05$, compared with untreated 2A-ALDH1A1-HT22 cells

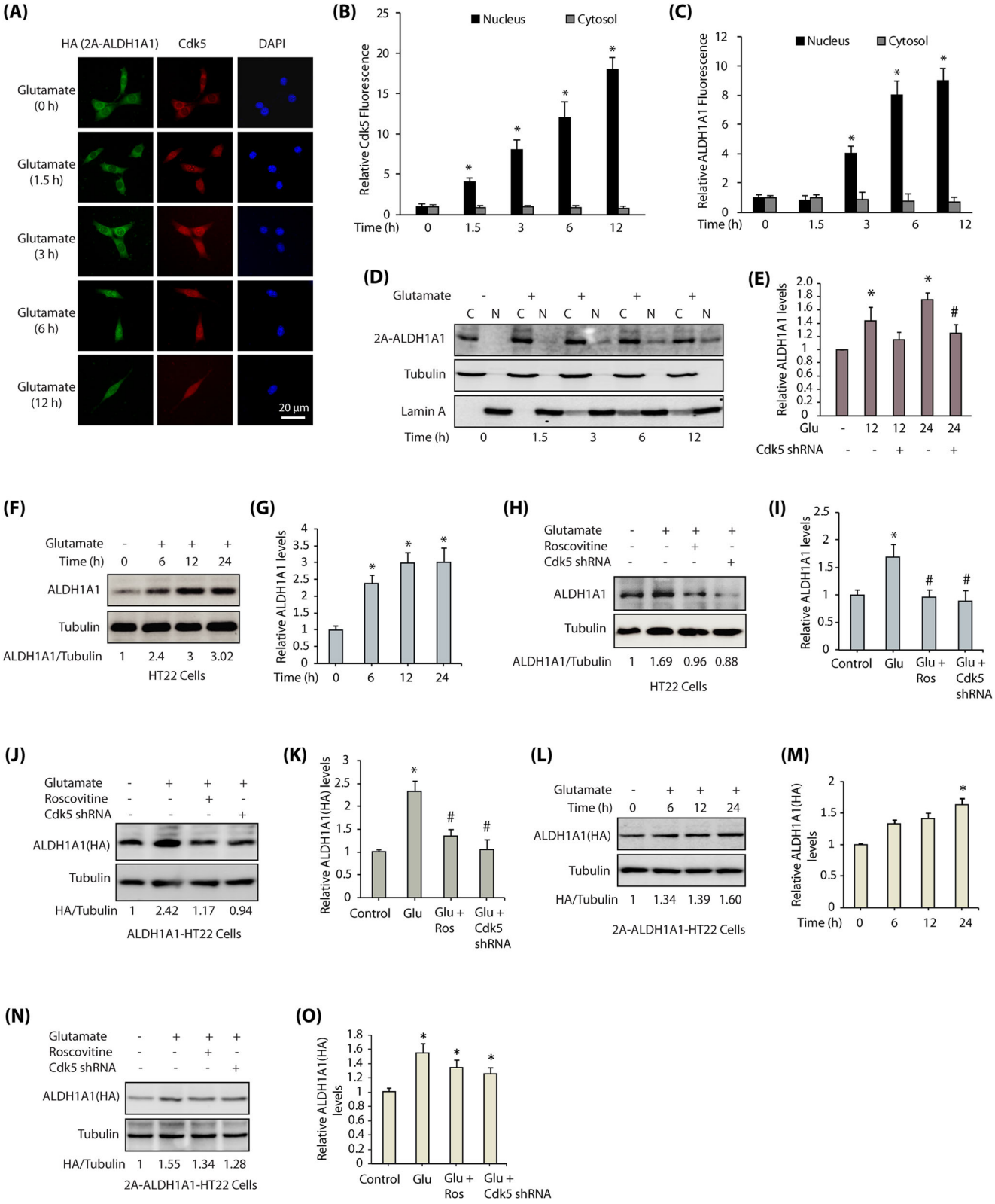

previous results [39]. Roscovitine also inhibits Cdk1 and Cdk2, both of which are critical for cell cycle in HT22 cells.

We next analyzed the impact of ALDH1A1 overexpression on cell viability. HT22, ALDH1A1-HT22, and 2A-ALDH1A1-HT22 cells exhibited similar cell viability under normal conditions (Fig. 6b). However, upon glutamate exposure, whereas HT22 cells revealed < 50% viability, ALDH1A1-expressing cells showed > 80% cell viability. In

contrast, 2A-ALDH1A1 expression offered little neuroprotection (Fig. 6b). Cdk5 depletion was highly and equally neuroprotective in all three glutamate-exposed cell lines as predicted. Thus, ectopic expression of ALDH1A1 is neuroprotective, which can counteract Cdk5-induced neurotoxicity to a significant extent. Notably, this finding indicated that Cdk5 in fact plays a neuroprotective role in glutamate-exposed cells by upregulating ALDH1A1. This result is in stark contrast with numerous known neurodegenerative pathways that are triggered by deregulated Cdk5.

Multifaceted Regulation of ALDH1A1 by Cdk5 in HT22 Cells: Neuroprotective and Neurodegenerative Roles of Cdk5

An increase in ALDH1A1 activity upon phosphorylation by Cdk5-p25 in vitro prompted us to investigate ALDH1A1 activity in HT22 cells exposed to glutamate. ALDH1A1 immunoprecipitated from HT22 cells displayed robust activity, which increased considerably after 12 h of glutamate treatment (Fig. 6c and Supplementary Fig. 4A). However, when ALDH1A1 was isolated after 24 h of glutamate treatment, it exhibited even lower activity than control HT22 cells. This result was unexpected as ALDH1A1 levels remain constant after 12 and 24 h of glutamate treatment (Fig. 4f, g). We also analyzed the activity of mutant ALDH1A1 isolated from 2A-ALDH1A1-HT22 cells (using HA antibody) upon glutamate treatment. As expected, 2A-ALDH1A1 was inactive, which underscores the importance of S75 and S274 residues for maintaining ALDH1A1 activity (Fig. 6c and Supplementary Fig. 4A).

We next investigated the impact of Cdk5 knockdown on ALDH1A1 activity in control and glutamate-treated cells. As before, exposure to glutamate increased ALDH1A1 activity in 12 h, but plummeted below the control levels in 24 h. Remarkably, Cdk5 knockdown prevented the increase in ALDH1A1 activity to a significant extent in 12-h glutamate-treated cells, but rescued ~50% of the decrease in ALDH1A1 activity in 24-h glutamate-treated cells (Fig. 6d and Supplementary Fig. 4B). This result was surprising as it suggested that Cdk5 is likely playing both a positive and a negative role in regulating ALDH1A1 activity in cells.

Cdk5 Inactivates ALDH1A1 Dehydrogenase Activity Via Sustained Oxidative Stress in Cells

To further delve into the mechanism of ALDH1A1 inactivation at 24 h, a potential role of oxidative stress in inactivating ALDH1A1 was examined in HT22 cells. Our previous studies have shown that Cdk5 promotes the formation of reactive oxygen species (ROS) in glutamate- and β-amyloid-treated HT22 cells and primary neurons. Cdk5 directly phosphorylates antioxidant proteins, peroxiredoxin-I (Prx-I) and peroxiredoxin-II (Prx-II), at T90 and T89 sites, respectively, which inactivate them, leading to increased oxidative stress [39].

Oxidative stress leads to lipid peroxidation, which generates over 200 different aldehydes, most of which are highly reactive and toxic [45]. ALDH enzymes including ALDH1A1 metabolize these aldehydes and thus mitigate oxidative/electrophilic stress in cells. However, as ALDH1A1 possesses a catalytic cysteine residue (C302), which is crucial for its dehydrogenase activity [44], we hypothesized that sustained oxidative stress triggered by Cdk5 deregulation may render ALDH1A1 inactive over time in glutamate-exposed HT22 cells. Glutamate treatment prevents cysteine uptake in HT22 cells, resulting in glutathione loss and increase in ROS levels [46].

To test this hypothesis, we eliminated ROS by transducing constitutively active TAT-peroxiredoxin-II-T89A (TAT-Prx-II-T89A) in neurotoxin-stimulated HT22 cells [39]. As Prx-II activity is eliminated by phosphorylation at T89 by Cdk5, Prx-II-T89A is constitutively active. TAT-RFP was used as a control, which showed no effect on any cellular event

Fig. 5 Cdk5-mediated phosphorylation of ALDH1A1 modulates its oligomeric state and dehydrogenase activity. **a** Monomeric ALDH1A1 displaying Cdk5 phosphorylation sites. S75 is present within the NAD^+ binding pocket (shown in cyan) and S274 is part of the catalytic site (highlighted in yellow). **b** Cdk5 increases ALDH1A1 enzymatic activity. Comparative spectrophotometric analysis of ALDH1A1 activity upon phosphorylation by Cdk5. ALDH1A1 activities with and without ATP and Cdk5 were used as controls. **c** Dephosphorylation of ALDH1A1 by calf-intestinal alkaline phosphatase (CIP) decreases its dehydrogenase activity. Each experiment was done at least three independent times. Representative data are shown. **d** ALDH1A1-phosphorylation- dead mutant have minimal enzymatic activity. **e** Phosphorylation of ALDH1A1 by Cdk5 triggers ALDH1A1 oligomers to dissociate to the monomeric form. **f** Average relative changes in tetramer and monomer abundance derived from three independent experiments. The intensities of tetramer and monomer at each time were normalized independently against time 0. $*p < 0.05$ versus monomer and $^{\#}p < 0.05$ versus tetramer at 15 and 30 min, respectively, from three independent experiments. **g** Average ratio of normalized monomer to tetramer as a function of time. To account for the large difference in tetramer and monomer abundance, the intensity of each band was normalized against the tetramer intensity at time zero and the ratio of monomer to tetramer was plotted as a function of time ($*p < 0.05$ at 15 and 30 min). **h** Activity staining of phosphorylation-induced ALDH1A1 monomer harbors high dehydrogenase activity. **i** Coomassie G-250 stain of **h**. **j** Quantification of oligomer-specific ALDH1A1 activity from three independent experiments ($*p < 0.05$ at 15 and 30 min) analyzed by two-way analysis of variance. Specifically, monomer and tetramer intensities of activity and Coomassie stain at 15 and 30 min of phosphorylation were normalized against the unphosphorylated tetramer control (basal activity); then, the normalized activity of each oligomer was divided by its respective normalized Coomassie signal to generate the plot. **k** Phos-tag staining of phosphorylated ALDH1A1 separated using native gel. **l** Coomassie G-250 stain of **k**. **m** Quantification of normalized Phos-tag intensities with respect to total protein levels from three independent experiments. Protein quantification was carried out in the same way as described for the activity assay ($*p < 0.05$ for monomer at 0 and 30 min analyzed by two-way analysis of variance). The green color denotes phosphorylation-specific signal

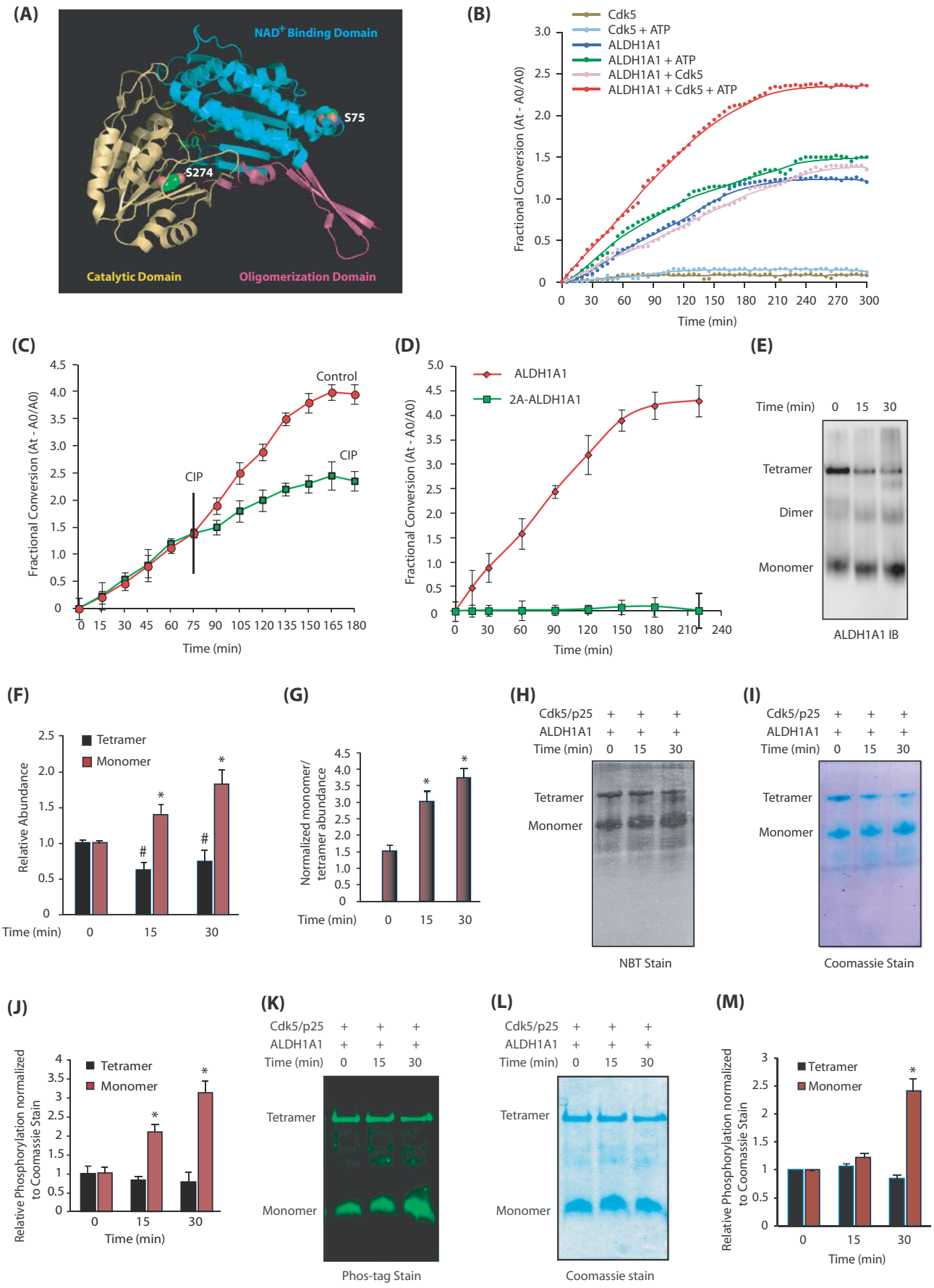
(A)
NAD+ Binding Domain
S75
S274
Catalytic Domain
Oligomerization Domain
(B)
Cdk5
Cdk5 + ATP
ALDH1A1
ALDH1A1 + ATP
ALDH1A1 + Cdk5
ALDH1A1 + Cdk5 + ATP
Fractional Conversion (At - A0/A0)
Time (min)
(C)
Control
CIP
CIP
Fractional Conversion (At - A0/A0)
Time (min)
(D)
ALDH1A1
2A-ALDH1A1
Fractional Conversion (At - A0/A0)
Time (min)
(E)
Time (min) 0 15 30
Tetramer
Dimer
Monomer
ALDH1A1 IB
(F)
Tetramer
Monomer
Relative Abundance
Time (min) 0 15 30
(G)
Normalized monomer/ tetramer abundance
Time (min) 0 15 30
(H)
Cdk5/p25 + + +
ALDH1A1 + + +
Time (min) 0 15 30
Tetramer
Monomer
NBT Stain
(I)
Cdk5/p25 + + +
ALDH1A1 + + +
Time (min) 0 15 30
Tetramer
Monomer
Coomassie Stain
(J)
Tetramer
Monomer
Relative Phosphorylation normalized to Coomassie Stain
Time (min)
(K)
Cdk5/p25 + + +
ALDH1A1 + + +
Time (min) 0 15 30
Tetramer
Monomer
Phos-tag Stain
(L)
Cdk5/p25 + + +
ALDH1A1 + + +
Time (min) 0 15 30
Tetramer
Monomer
Coomassie stain
(M)
Tetramer
Monomer
Relative Phosphorylation normalized to Coomassie Stain
Time (min)

Fig. 6 Upregulation of ALDH1A1 by Cdk5 is initially neuroprotective and finally neurodegenerative. **a** Cdk5 depletion provides neuroprotection upon glutamate exposure. Scrambled-shRNA-infected Cdk5-shRNA- or ALDH1A1-shRNA-infected or roscovitine-exposed HT22 cells were treated with glutamate for 24 h. Cell viability was examined using an MTT assay. $*p < 0.05$, compared with untreated HT22 cells. **b** ALDH1A1 overexpression rescue cells from glutamate-induced neurotoxicity. HT22, ALDH1A1-HT22, and 2A-ALDH1A1-HT22 cells were treated with glutamate, roscovitine, and Cdk5 shRNA and cell viability tested by using an MTT assay. **c** Glutamate treatment increased ALDH1A1 activity in HT22 cells while the phosphorylation-resistant mutant cells have diminished enzymatic activity. HT22 and 2A-ALDH1A1-HT22 cells were treated with glutamate for 12 and 24 h. ALDH1A1 was immunoprecipitated using ALDH1A1 and HA antibody, respectively, and enzyme activity was performed as described in the "Materials and Methods" section. **d** Cdk5 depletion partially prevents the increase in ALDH1A1 activity in 12-h glutamate-treated cells, but rescues ~50% of the decrease in ALDH1A1 activity in 24-h glutamate-treated cells. HT22- and Cdk5-shRNA-treated-HT22 cells were exposed to glutamate for 12 and 24 h. ALDH1A1 was isolated and its activity analyzed. **e** Elimination of oxidative stress restores ALDH1A1 activity to a significant extent. First set of HT22 cells was treated with glutamate for 12 and 24 h. Second set was pretreated with glutamate for 12 and 16 h, followed by treatment with 200-nM TAT-fused peroxiredoxin-II-T89A for the next 12 and 8 h, respectively. TAT-fused peroxiredoxin-II-T89A protein was purified fresh and added every 4 h. TAT-fusion red fluorescent protein (TAT-RFP) was used as a control. ALDH1A1 immune complex was isolated and its dehydrogenase activity determined as described in the "Materials and Methods" section. **f** DTT treatment is beneficial for ALDH1A1 enzymatic activity initially. HT22 cells were treated with glutamate for 12 and 24 h. ALDH1A1 was immunoprecipitated using ALDH1A1 antibody, and enzyme activity was performed with or without 10 mM DTT in reaction buffers as described in the "Materials and Methods" section. **g** Eliminating oxidative stress affects ALDH1A1 level. HT22 cells were treated as described in **e** and ALDH1A1 levels analyzed. **h** ALDH1A1 protein levels in HT22 cells in response to glutamate treatment with or without TAT-Prx-II (T89A) pretreatment. Graphical results are mean ± SEM of three independent experiments. $*p < 0.05$, compared with untreated HT22 cells, and $^{\#}p < 0.05$, compared with only glutamate-treated HT22 cells. **i** Exposure to sub-lethal concentration of H_2O_2 increases ALDH1A1 protein levels. HT22 cells were treated with varying concentrations of H_2O_2 for 12 h and ALDH1A1 levels analyzed. **j** ALDH1A1 mRNA increases on exposure to glutamate treatment. HT22 cells were exposed to 5 mM glutamate and ALDH1A1 mRNA levels analyzed using semi-quantitative PCR after 12 and 24 h of treatments. **k** ALDH1A1 mRNA levels in HT22 cells in response to glutamate treatment for 12 and 24 h. Graphical results are mean ± SEM of three independent experiments. $*p < 0.05$, compared with untreated HT22 cells. **l** Exposure to sub-lethal concentration of H_2O_2 increases ALDH1A1 mRNA levels in HT22 cells. **m** Exposure to sub-lethal concentration of H_2O_2 increases ALDH1A1 mRNA levels. Graphical results are mean ± SEM of three independent experiments. $*p < 0.05$, compared with untreated HT22 cells. **n** Glutamate exposure decreases ALDH1A1 ubiquitylation in a Cdk5-dependent manner. 6× His ubiquitin was expressed in HT22 cells, followed by glutamate treatment for 12 h in the presence and absence of Cdk5 shRNA. ALDH1A1 was immunoprecipitated and potential ubiquitylation analyzed using 6× His antibody. Each experiment was done at least three independent times. Representative data are shown. **o** HA-tagged wild-type ALDH1A1 displays less ubiquitylation in response to glutamate treatment. HA-ALDH1A1-HT22 cells were treated similarly as described above, and ubiquitylated proteins were isolated using HA antibody and analyzed. Each experiment was done at least three independent times. Representative data are shown. **p** 2A-ALDH1A1 is resistant to Cdk5-dependent protection to ubiquitylation. 2A-ALDH1A1-HT22 cells were treated similarly, and ubiquitylated proteins were isolated using HA antibody and analyzed. Each experiment was done at least three independent times. Representative data are shown

investigated. Glutamate exposure for 12 h showed a robust increase in ALDH1A1 activity, while 24 h treatment revealed substantially diminished activity (Fig. 6e and Supplementary Fig. 4C). However, when TAT-Prx-II (T89A) was added after 16 h of glutamate treatment and ALDH1A1 activity monitored after another 8 h (total 24 h of glutamate treatment), it significantly rescued ALDH1A1 activity (Fig. 6e and Supplementary Fig. 4C). Likewise, when TAT-Prx-II (T89A) was transduced after 12 h of glutamate treatment and incubated for another 12 h (total 24 h of treatment), it rescued ALDH1A1 activity to a higher degree (Fig. 6e and Supplementary Fig. 4C). These results show that although ALDH1A1 levels remain constant at 12 and 24 h of glutamate treatments, Cdk5-induced oxidative stress renders ALDH1A1 inactive, abolishing its neuroprotective function.

Persistent Neurotoxic Conditions Irreversibly Impairs ALDH1A1 Activity

We examined whether oxidation of catalytic cysteine was inactivating ALDH1A1 under neurotoxic conditions. ALDH1A1 was isolated from glutamate-treated HT22 cells exposed for 12 and 24 h, and their catalytic activity was examined in the absence or presence of DTT in vitro. Addition of DTT slightly improved the dehydrogenase activity of ALDH1A1 isolated after 12 h of treatment; however, it could not salvage the activity of ALDH1A1 isolated after 24 h of treatment (Fig. 6f and Supplementary Fig. 4D). These results show that ALDH1A1 is irreversibly damaged by other ROS-induced injuries upon prolonged exposure.

Paradoxically Cdk5-Induced Oxidative Stress Contributes to ALDH1A1 Upregulation at Transcriptional Level

Many studies show a detoxifying role of ALDH1A1 in mitigating oxidative stress-induced injury; however, to our knowledge, no study has shown ALDH1A1 upregulation in cells exposed to oxidative stress. To examine whether oxidative stress generated by glutamate alters ALDH1A1 levels, we exposed HT22 cells to glutamate for 12 h, followed by the addition of TAT-Prx-II (T89A) for another 12 h. Eliminating ROS using TAT-Prx-II for the last 12 h of glutamate treatment resulted in ~30% decrease in ALDH1A1 levels, compared to glutamate-treated cells. Similarly, ~15% decrease in ALDH1A1 levels was observed when TAT-Prx-II was added in HT22 cells after 16 h of glutamate treatment for another 8-h incubation. This result suggested that abrogation of oxidative

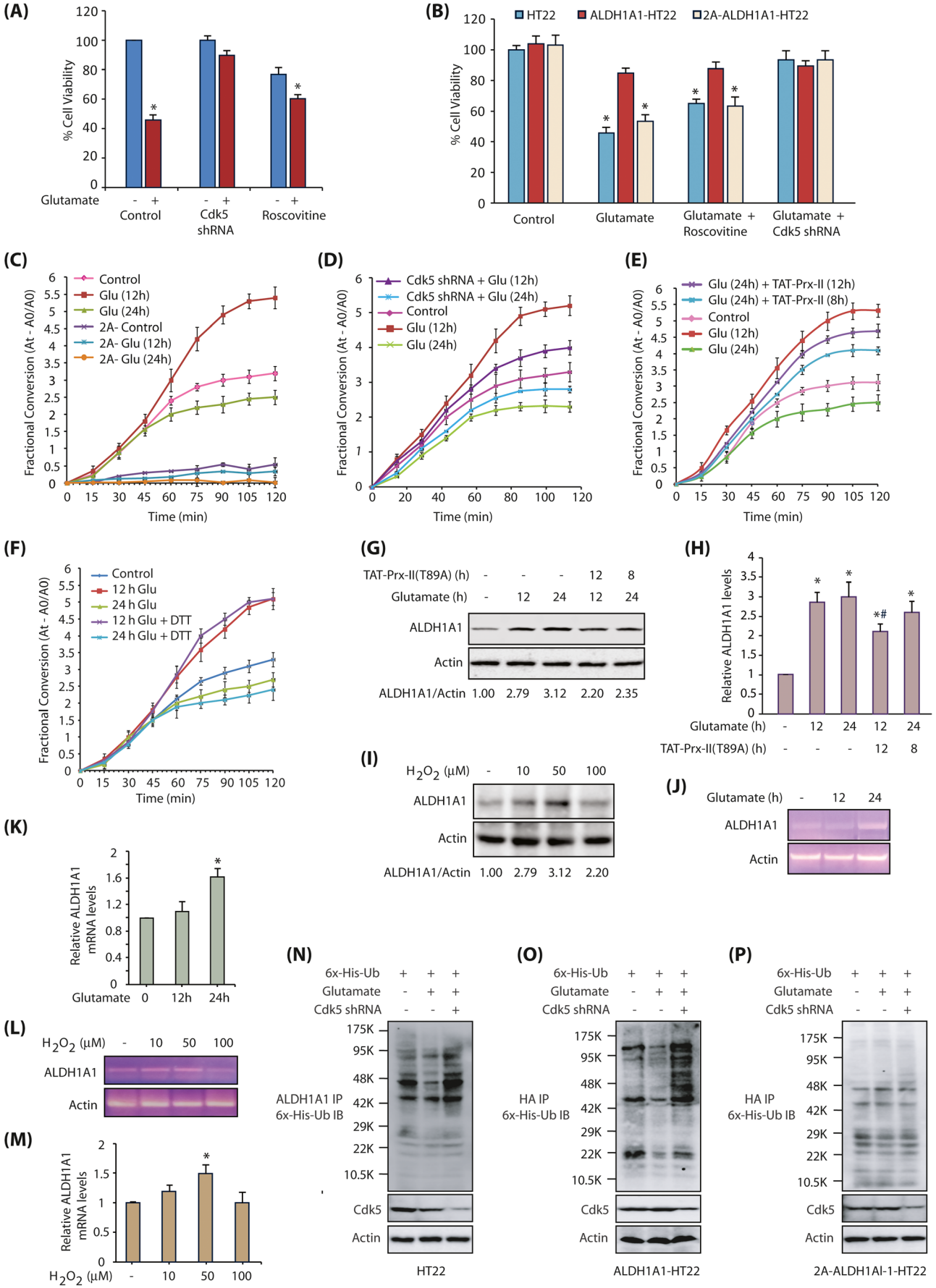
(A)
% Cell Viability
Glutamate
Control
Cdk5 shRNA
Roscovitine
(B)
HT22
ALDH1A1-HT22
2A-ALDH1A1-HT22
% Cell Viability
Control
Glutamate
Glutamate + Roscovitine
Glutamate + Cdk5 shRNA
(C)
Control
Glu (12h)
Glu (24h)
2A- Control
2A- Glu (12h)
2A- Glu (24h)
Fractional Conversion (At - A0/A0)
Time (min)
(D)
Cdk5 shRNA + Glu (12h)
Cdk5 shRNA + Glu (24h)
Control
Glu (12h)
Glu (24h)
Fractional Conversion (At - A0/A0)
Time (min)
(E)
Glu (24h) + TAT-Prx-II (12h)
Glu (24h) + TAT-Prx-II (8h)
Control
Glu (12h)
Glu (24h)
Fractional Conversion (At - A0/A0)
Time (min)
(F)
Control
12 h Glu
24 h Glu
12 h Glu + DTT
24 h Glu + DTT
Fractional Conversion (At - A0/A0)
Time (min)
(G)
TAT-Prx-II(T89A) (h) - - - 12 8
Glutamate (h) - 12 24 12 24
ALDH1A1
Actin
ALDH1A1/Actin 1.00 2.79 3.12 2.20 2.35
(H)
Relative ALDH1A1 levels
Glutamate (h) - 12 24 12 24
TAT-Prx-II(T89A) (h) - - - 12 8
(I)
H2O2 (μM) - 10 50 100
ALDH1A1
Actin
ALDH1A1/Actin 1.00 2.79 3.12 2.20
(J)
Glutamate (h) - 12 24
ALDH1A1
Actin
(K)
Relative ALDH1A1 mRNA levels
Glutamate 0 12h 24h
(L)
H2O2 (μM) - 10 50 100
ALDH1A1
Actin
(M)
Relative ALDH1A1 mRNA levels
H2O2 (μM) - 10 50 100
(N)
6x-His-Ub + + +
Glutamate - + +
Cdk5 shRNA - - +
175K
95K
48K
42K
29K
22K
10.5K
ALDH1A1 IP
6x-His-Ub IB
Cdk5
Actin
HT22
(O)
6x-His-Ub + + +
Glutamate - + +
Cdk5 shRNA - - +
HA IP
6x-His-Ub IB
Cdk5
Actin
ALDH1A1-HT22
(P)
6x-His-Ub + + +
Glutamate - + +
Cdk5 shRNA - - +
HA IP
6x-His-Ub IB
Cdk5
Actin
2A-ALDH1Al-1-HT22

stress reduces ALDH1A1 levels (Fig. 6g). Figure 6h shows the effect of ROS elimination on ALDH1A1 levels from three independent experiments.

To further confirm that glutamate-induced oxidative stress is contributing to ALDH1A1 upregulation, we treated HT22 cells with 10, 50, and 100 μM of hydrogen peroxide for 12 h and analyzed the levels of ALDH1A1. Exposure to 10 and 50 μM H_2O_2 increased the levels of ALDH1A1, confirming that oxidative stress increases ALDH1A1 levels (Fig. 6i). As 100 μM H_2O_2 was toxic to cells, the decrease in ALDH1A1 levels was expected.

Although the increase in ALDH1A1 level was modest but statistically significant in glutamate or oxidative stress-induced cells, we next examined whether this increase was transcriptionally regulated. HT22 cells were either exposed to glutamate (12 and 24 h) or H_2O_2 (12 h) and ALDH1A1 mRNA levels analyzed using semi-quantitative PCR. Glutamate treatment showed minimal increase in ALDH1A1 mRNA levels after 12 h, but showed almost 1.5-fold increase after 24 h of glutamate treatment (Fig. 6j, k). Similarly, we observed approximately 1.5-fold enhancement in ALDH1A1 mRNA levels in 50-μM H_2O_2-exposed cells, but not at higher toxic concentration (Fig. 6l, m). These data suggest that Cdk5-mediated oxidative stress in glutamate-exposed cells contributes to ALDH1A1 mRNA upregulation at the transcriptional level as was observed before (Fig. 4e).

Cdk5-Mediated Phosphorylation of ALDH1A1 Stabilizes Its Protein Level

As the decrease in ALDH1A1 levels upon TAT-Prx-II transduction was ~30% compared to glutamate-treated cells (Fig. 6g, h), it suggested that glutamate-induced ROS upregulates ALDH1A1 to some extent, but does not fully account for Cdk5-mediated upregulation of ALDH1A1 (which was ~3-fold; Fig. 4f). Therefore, we investigated whether Cdk5-mediated phosphorylation of ALDH1A1 contributes to its increased stability. The 6× His ubiquitin was expressed in HT22, ALDH1A1-HT22, and 2A-ALDH1A1-HT22 cells, followed by glutamate treatment for 12 h. ALDH1A1 was immunoprecipitated using either ALDH1A1 antibody (Fig. 6n) or using HA antibody (Fig. 6o, p) and potential ubiquitylation analyzed. As shown in Fig. 6n, glutamate treatment resulted in reduced ubiquitylation of ALDH1A1 (compare lanes 1 and 2), which was inhibited upon Cdk5 depletion (compare lanes 2 and 3). Similar results were obtained in HA-tagged ALDH1A1-HT22 cells upon glutamate treatment, confirming that Cdk5 promotes ALDH1A1 stabilization in glutamate-exposed HT22 cells (Fig. 6o). In contrast, HA-tagged 2A-ALDH1A1 cells showed almost similar level of ubiquitylation in control, glutamate-treated, and glutamate- and Cdk5-shRNA-treated cells, thereby suggesting that Cdk5-mediated phosphorylation of ALDH1A1 contributes to increased stability of ALDH1A1 (Fig. 6p).

Collectively, these data reveal multi-layered regulation of ALDH1A1 by Cdk5 in neurotoxin-exposed neuronal cells. First, Cdk5-induced oxidative stress contributes to an increase in ALDH1A1 levels via increased transcription. Second, Cdk5-mediated direct phosphorylation of ALDH1A1 prevents its ubiquitylation leading to increased protein levels. Third, Cdk5-dependent phosphorylation of ALDH1A1 increases its dehydrogenase activity by altering its oligomeric state. Fourth, persistent oxidative stress triggered by Cdk5 deregulation impacts ALDH1A1 enzymatic activity rendering its inactive.

Thus, these data highlight contrasting roles of Cdk5 in the regulation of ALDH1A1. Initially, Cdk5 attempts to mitigate ensuing oxidative stress by upregulating ALDH1A1 via phosphorylation and paradoxically by increasing oxidative stress. However, later, sustained oxidative stress generated by Cdk5 inhibits ALDH1A1 activity, leading to neurotoxicity. Thus, it appears that Cdk5 is initially neuroprotective and eventually neurotoxic in AD pathogenesis.

ALDH1A1 Upregulation Is Highly Neuroprotective in Mature Primary Cortical Neurons Under Excitotoxic Conditions

To determine a potential role of Cdk5 in regulating ALDH1A1 signaling under more pathologically relevant conditions, we chose 100 μM glutamate as the stimulus to induce excitotoxicity in mature mouse primary cortical neurons [47]. Excitotoxicity resulted in ~60% loss in neuronal viability over 24 h, which was largely prevented by Cdk5 depletion (Fig. 7a). Roscovitine partially prevented loss of cell viability, consistent with the results obtained in HT22 cells (Fig. 6a). Importantly, ALDH1A1 upregulation mostly prevented this loss, which highlights its critical neuroprotective role under neurotoxic conditions (Fig. 7b).

Cdk5 Regulates ALDH1A1 Subcellular Localization in Mature Primary Cortical Neurons Upon Excitotoxicity

To investigate the regulation of ALDH1A1 under excitotoxic conditions, we analyzed its subcellular localization. Exposure of mature mouse primary cortical neurons to glutamate led to a robust increase in the nuclear translocation of both Cdk5 and ALDH1A1, which was inhibited by roscovitine and Cdk5 depletion (Fig. 7c–e). Cdk5 inhibition or depletion also resulted in significant shrinkage of neurites and axon, which is consistent with previous findings highlighting a key role of Cdk5 in neuronal differentiation in primary cortical neurons (Fig. 7c, e) [48].

ALDH1A1 Is Upregulated at mRNA and Protein Levels in Mature Primary Cortical Neurons Under Excitotoxic Conditions

Excitotoxicity also caused a slight increase in ALDH1A1 transcription at 12 h (1.2-fold), which increased to ~1.5-fold in 24 h (Fig. 7f), similar to that obtained using HT22 cells (Fig. 4e). Cdk5 ablation inhibited the increase in ALDH1A1 transcription. Figure 7g shows average ALDH1A1 mRNA levels in primary cortical neurons upon excitotoxicity from three independent experiments, determined using semi-quantitative PCR. We also quantified ALDH1A1 transcript levels in primary cortical neurons exposed to excitotoxicity using real-time qPCR, which further confirmed that the modest increase in ALDH1A1 transcript levels is regulated by Cdk5 (Fig. 7h).

ALDH1A1 protein levels were also examined in glutamate-exposed primary neurons. Similar to HT22 cells, glutamate treatment led to an ~3.3-fold increase in ALDH1A1 levels in 12 h, which remained constant after 24 h (Fig. 7i). Figure 7j displays the alterations in ALDH1A1 levels when exposed to excitotoxic conditions from three independent experiments. Both Cdk5 knockdown and inhibition largely prevented this increase in ALDH1A1 levels (Fig. 7k, l).

Cdk5 Initially Increases ALDH1A1 Enzymatic Activity Upon Excitotoxicity

ALDH1A1 activity was subsequently examined in glutamate-exposed primary cortical neurons, which revealed a robust increase in ALDH1A1 activity at 12 h, which declined below control levels in 24 h, similar to the results obtained in HT22 cells (Fig. 7m). Cdk5 was next knocked down, followed by 12 h of glutamate treatment. ALDH1A1 immune complex was isolated and its activity analyzed, which revealed similar activity as that of the control neurons (Fig. 7m and Supplementary Fig. 5A). These results indicate that Cdk5 is crucial for the increase in ALDH1A1 activity observed upon glutamate exposure in primary cortical neurons. As Cdk5 depletion has opposing consequences on ALDH1A1 levels and activity, it was expected that ALDH1A1 activity remains unaffected under excitotoxic conditions when Cdk5 was knocked down. As noted before, at one end, Cdk5 depletion prevents the increase in ALDH1A1 levels and activity, whereas at the other end, it also prevents the inactivation of ALDH1A1 at the later stage under neurotoxic conditions. Most importantly, collectively, these results show that ALDH1A1 regulation by Cdk5 is similar in primary cortical neurons exposed to excitotoxicity and glutamate-exposed HT22 cells.

Decrease in ALDH1A1 Activity at Later Stages Is Partially Due to Increased Oxidative Stress

To delve deeper into the mechanism of neurotoxicity, we investigated whether increasing ROS was contributing to ALDH1A1 inactivation at a later stage. Primary neurons were treated with glutamate for 12 h, and then treated with TAT-Prx-II (89A) for another 12 h (total 24 h of glutamate treatment, purple line; Fig. 7n and Supplementary Fig. 5B), which significantly rescued its activity. However, when TAT-Prx-II (89A) was added after 16 h of glutamate treatment (total 8 h of TAT-Prx-II treatment, light blue line; Fig. 7n), it showed little impact on ALDH1A1 activity. These results suggest that oxidative stress is an important factor in ALDH1A1 inactivation.

To investigate whether oxidation of catalytic cysteine was responsible for its diminished activity under neurotoxic conditions, we isolated ALDH1A1 from glutamate-exposed neurons for 12 and 24 h and determined their catalytic activity with and without DTT in vitro. DTT improved the activity of ALDH1A1 isolated after 12 h of treatment, but did not rescue ALDH1A1 activity isolated after 24 h of treatment (Fig. 7o and Supplementary Fig. 5C). These results show that initial oxidative damage to ALDH1A1 is minor and reversible; however, at later stage, DTT is unable to rescue ALDH1A1 activity, presumably due to other ROS-induced impairments (Fig. 7o and Supplementary Fig. 5C).

ALDH1A1 Is Also a Physiological Target of Cdk5

Thus far, our results show that ALDH1A1 is regulated by Cdk5 under neurotoxic conditions. Deregulated Cdk5 increases ALDH1A1 activity and levels, which confers neuroprotection initially; however, sustained neurotoxic conditions eventually damage ALDH1A1 irreversibly contributing to further toxicity. Since ALDH1A1 signaling is crucial for normal brain homeostasis, we envisioned that Cdk5 may also regulate ALDH1A1 under physiological conditions.

To test this hypothesis, we chose a physiologically relevant primary neuron model. Primary cortical neurons isolated from E17/E18 embryos show little Cdk5 level and activity; however, when they are grown in vitro (days in vitro (DIV)) for a couple of weeks, they develop morphologically and functionally, which is accompanied by concomitant increase in Cdk5 and p35 levels, resulting in increased Cdk5 activity. Cdk5 knockdown inhibits neuronal survival, neuronal differentiation, neuronal migration, dendrite formation, and ultimately their maturation under physiological conditions. Therefore, development of primary cortical neurons in vitro provides an apt model to test whether Cdk5 regulates ALDH1A1 under normal physiological conditions.

We initially measured Cdk5 kinase activity in primary cortical neurons isolated from DIV1, DIV6, and DIV13. Cdk5

activity increased 6-fold on DIV6 and 16-fold on DIV14, compared to DIV1 (Fig. 8a). In parallel, we also investigated Cdk5, p35, and ALDH1A1 levels in DIV6 and DIV14 primary neurons, which revealed more than 5-fold increase in Cdk5 and p35 levels (Fig. 8b). ALDH1A1 levels also increased > 2-fold on DIV14, suggesting that ALDH1A1 upregulation in maturing neurons may be crucial for normal neuronal functions. Most importantly, Cdk5 knockdown in DIV14 primary cortical neurons reduced ALDH1A1 levels, confirming that Cdk5 also regulates ALDH1A1 under physiological conditions.

ALDH1A1 Levels Increase With Disease Severity in AD Clinical Specimens

To investigate the clinical significance of our findings, we examined ALDH1A1 levels in human AD and age-matched control brain tissues. We procured the tissues from prefrontal cortex area 9 (Brodmann's area 9), a prefrontal association region located in the superior frontal gyrus of the brain, which is severely affected in AD [49]. These neurons are highly vulnerable in AD and their loss strongly correlates with the severity of the disease, with more than 90% loss occurring at the end stages of AD [50]. ALDH1A1 levels were analyzed in tissues obtained from AD patients at mild ($n = 1$), moderate stage ($n = 2$), and severe stage ($n = 2$) along with age-matched controls ($n = 3$). Although we were able to obtain a few specimens, ALDH1A1 levels did not show significant change among normal, mild, and moderate AD tissues (Fig. 8c). However, ALDH1A1 levels showed relatively higher levels in both of the severe cases, suggesting that ALDH1A1 upregulation may be a compensatory mechanism to combat ensuing oxidative stress in AD pathogenesis. Figure 8d shows the average ALDH1A1 levels in normal, mild, moderate, and severe AD specimens from three independent experiments.

ALDH1A1 Activity Initially Rise and Later Decline With Increased Disease Severity in AD Clinical Specimens

These results prompted us to investigate ALDH1A1 activity in these tissues, which may be regulated independently of their levels in AD. ALDH1A1 was isolated from each of these specimens and its dehydrogenase activity examined. Interestingly, mild ($n = 1$) and moderate stage ($n = 2$) specimens showed increased activity compared to age-matched controls ($n = 3$), despite similar levels, suggesting that ALDH1A1 activation indeed occurs at the initial stages of the disease. Furthermore, ALDH1A1 activity was severely diminished in severe AD cases, suggesting that neurotoxic conditions destroy the activity of ALDH1A1 despite the increased levels (Fig. 8e, f).

To further confirm these results, we procured another cohort of 22 human clinical specimens (Brodmann area 9),

Fig. 7 Cdk5-ALDH1A1 signaling in primary neurons. **a** Inhibition and ablation of Cdk5 inhibits neurotoxicity in primary cortical neurons. Cdk5-shRNA-infected primary neurons (30 h) were treated with glutamate (24 h). Cell viability was tested by an MTT assay. $^{*}p < 0.05$, compared with untreated neurons. **b** Overexpression of ALDH1A1 prevents neurotoxicity in primary cortical neurons. ALDH1A1 overexpressed primary neurons (30 h) were treated with glutamate (24 h). Cell viability was tested by MTT assay. $^{*}p < 0.05$, compared with untreated neurons. **c** Glutamate exposure triggers nuclear translocation of ALDH1A1 in a Cdk5-dependent manner. Primary cortical neurons were treated with glutamate (100 μM) for 12 h in the presence or absence of roscovitine (10 μM), followed by immunostaining with Cdk5 and ALDH1A1 antibodies. **d** Quantification of the subcellular localization of ALDH1A1 in the cell nucleus versus the cytoplasm. The graphs show the mean ± SEM of the relative fluorescence intensity with respect to control cells. $^{*}p < 0.05$ versus nucleus fraction control analyzed by two-way analysis of variance. **e** Cdk5 depletion inhibits nuclear translocation of ALDH1A1. Primary cortical neurons were treated with glutamate (100 μM) for 12 h in the presence or absence of Cdk5 shRNA, followed by immunostaining with Cdk5 and ALDH1A1 antibodies. **f** Primary cortical neurons were treated with glutamate for 12 and 24 h, in the presence and absence of Cdk5 shRNA, and then, the total levels of ALDH1A1 mRNA were analyzed using semi-quantitative RT-PCR. **g** ALDH1A1 mRNA levels in primary cortical neurons in response to glutamate treatment with or without Cdk5 shRNA. Graphical results are mean ± SEM of three independent experiments. $^{*}p < 0.05$, compared with untreated primary cortical neurons. $^{\#}p < 0.05$, compared with only glutamate-treated neurons. **h** Primary cortical neurons were treated similarly as described for **f**, **g**, and total mRNA levels of ALDH1A1 were detected by real-time qPCR. Expression levels are normalized to the expression of actin. Results are mean ± SEM of three independent experiments. $^{*}p < 0.05$, compared with untreated neurons. $^{\#}p < 0.05$, compared with only glutamate-treated neurons. **i** Glutamate treatment increases ALDH1A1 protein levels in primary cortical neurons in a time-dependent manner. Primary cortical neurons were treated with glutamate for 0–24 h and the total levels of ALDH1A1 analyzed. **j** Average relative ratios of ALDH1A1 band intensities to alpha-tubulin band intensities upon glutamate treatment as obtained from three independent experiments. $^{*}p < 0.05$, compared with untreated primary neurons. **k** Glutamate treatment increases ALDH1A1 protein levels in primary cortical neurons in a Cdk5-dependent manner. ALDH1A1 levels were analyzed upon glutamate (12 h), roscovitine, and Cdk5 shRNA treatments. **l** ALDH1A1 protein levels in primary cortical neurons in response to glutamate treatment with or without roscovitine and Cdk5 shRNA. Graphical results are mean ± SEM of three independent experiments. $^{*}p < 0.05$, compared with untreated primary neurons, and $^{\#}p < 0.05$, compared with only glutamate-treated primary neurons. **m** ALDH1A1 enzyme activity in primary cortical neurons in response to glutamate treatment with or without Cdk5 shRNA. **n** Removal of oxidative stress restores ALDH1A1 activity to a significant extent. Primary cortical neurons were either treated with glutamate for 12 and 24 h or were pretreated with glutamate for 12 and 16 h, followed by subsequent treatment with 200-nM TAT-fused peroxiredoxin-II-T89A for the next 12 and 8 h, respectively. TAT-fused peroxiredoxin-II-T89A protein was purified fresh and added every 4 h. TAT-fusion red fluorescent protein (TAT-RFP) was used as a control. ALDH1A1 immune complex was isolated, and its dehydrogenase activity was determined as described in the "Materials and Methods" section. **o** DTT treatment is beneficial for ALDH1A1 enzymatic activity initially. Primary cortical neuron cells were treated with glutamate for 12 and 24 h. ALDH1A1 was immunoprecipitated using ALDH1A1 antibody, and enzyme activity was performed with or without 10 mM DTT in reaction buffers as described in the "Materials and Methods" section

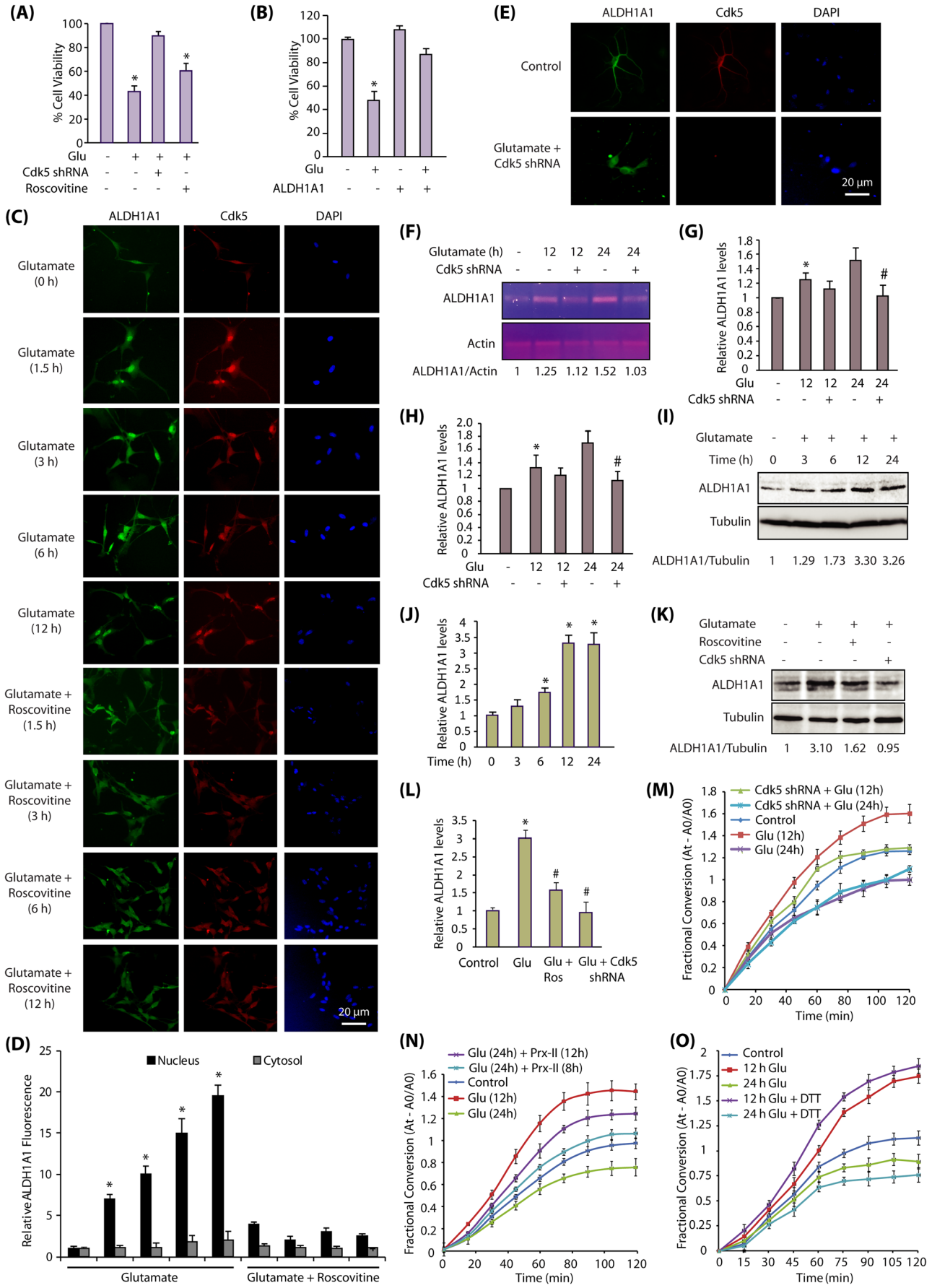
(A)
% Cell Viability
Glu
Cdk5 shRNA
Roscovitine
(B)
% Cell Viability
Glu
ALDH1A1
(E)
ALDH1A1
Cdk5
DAPI
Control
Glutamate + Cdk5 shRNA
20 μm
(C)
ALDH1A1
Cdk5
DAPI
Glutamate (0 h)
Glutamate (1.5 h)
Glutamate (3 h)
Glutamate (6 h)
Glutamate (12 h)
Glutamate + Roscovitine (1.5 h)
Glutamate + Roscovitine (3 h)
Glutamate + Roscovitine (6 h)
Glutamate + Roscovitine (12 h)
20 μm
(F)
Glutamate (h)
Cdk5 shRNA
ALDH1A1
Actin
ALDH1A1/Actin 1 1.25 1.12 1.52 1.03
(G)
Relative ALDH1A1 levels
Glu
Cdk5 shRNA
(H)
Relative ALDH1A1 levels
Glu
Cdk5 shRNA
(I)
Glutamate
Time (h)
ALDH1A1
Tubulin
ALDH1A1/Tubulin 1 1.29 1.73 3.30 3.26
(J)
Relative ALDH1A1 levels
Time (h)
(K)
Glutamate
Roscovitine
Cdk5 shRNA
ALDH1A1
Tubulin
ALDH1A1/Tubulin 1 3.10 1.62 0.95
(L)
Relative ALDH1A1 levels
Control
Glu
Glu + Ros
Glu + Cdk5 shRNA
(M)
Cdk5 shRNA + Glu (12h)
Cdk5 shRNA + Glu (24h)
Control
Glu (12h)
Glu (24h)
Fractional Conversion (At - A0/A0)
Time (min)
(D)
Nucleus
Cytosol
Relative ALDH1A1 Fluorescence
Glutamate
Glutamate + Roscovitine
(N)
Glu (24h) + Prx-II (12h)
Glu (24h) + Prx-II (8h)
Control
Glu (12h)
Glu (24h)
Fractional Conversion (At - A0/A0)
Time (min)
(O)
Control
12 h Glu
24 h Glu
12 h Glu + DTT
24 h Glu + DTT
Fractional Conversion (At - A0/A0)
Time (min)

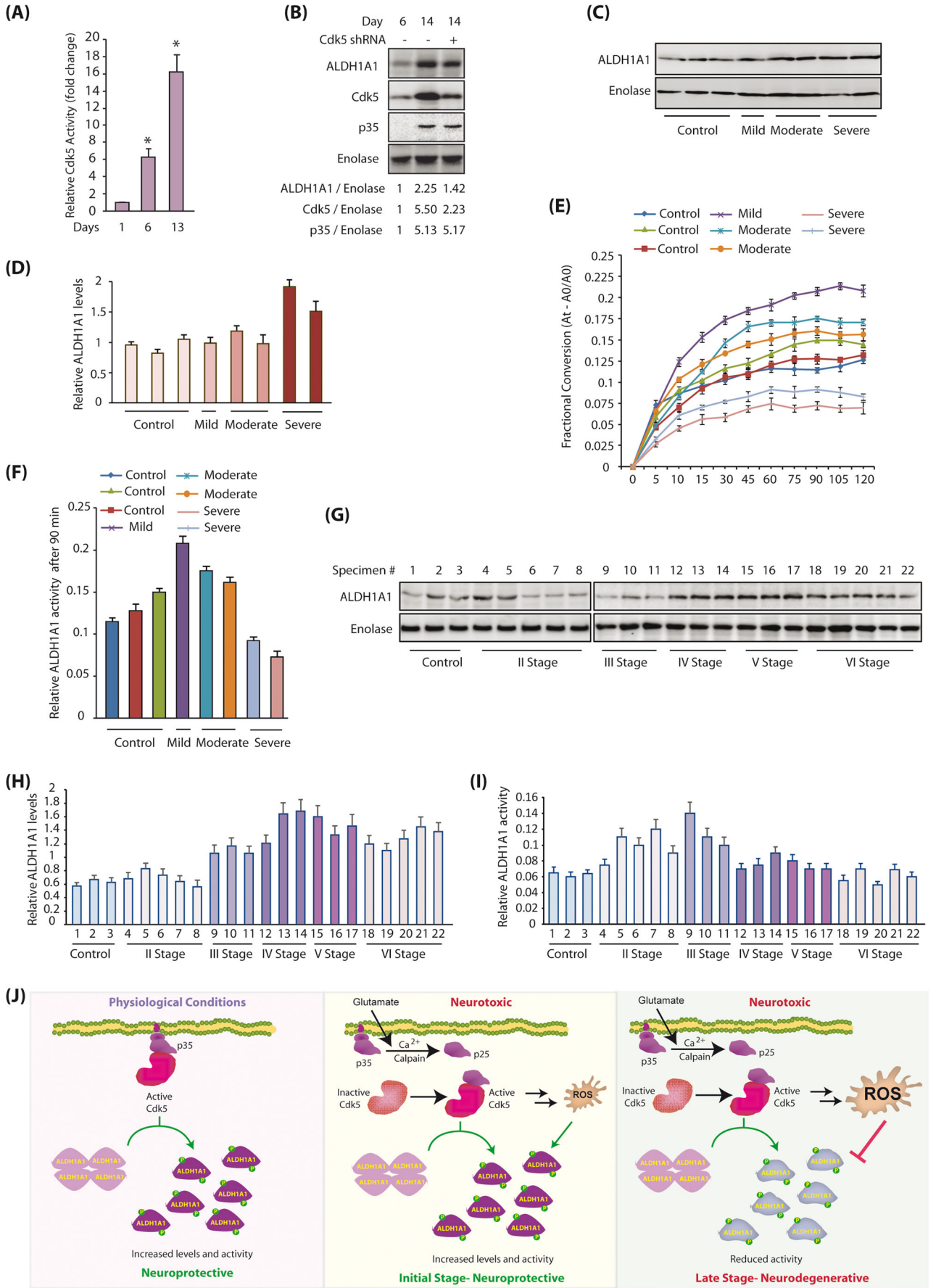
(A)
Relative Cdk5 Activity (fold change)
Days 1 6 13
(B)
Day 6 14 14
Cdk5 shRNA - - +
ALDH1A1
Cdk5
p35
Enolase
ALDH1A1 / Enolase 1 2.25 1.42
Cdk5 / Enolase 1 5.50 2.23
p35 / Enolase 1 5.13 5.17
(C)
ALDH1A1
Enolase
Control Mild Moderate Severe
(D)
Relative ALDH1A1 levels
Control Mild Moderate Severe
(E)
Control Mild Severe
Control Moderate Severe
Control Moderate
Fractional Conversion (At - A0/A0)
(F)
Control Moderate
Control Moderate
Control Severe
Mild Severe
Relative ALDH1A1 activity after 90 min
Control Mild Moderate Severe
(G)
Specimen # 1 2 3 4 5 6 7 8 9 10 11 12 13 14 15 16 17 18 19 20 21 22
ALDH1A1
Enolase
Control II Stage III Stage IV Stage V Stage VI Stage
(H)
Relative ALDH1A1 levels
Control II Stage III Stage IV Stage V Stage VI Stage
(I)
Relative ALDH1A1 activity
Control II Stage III Stage IV Stage V Stage VI Stage
(J)
Physiological Conditions
p35
Active Cdk5
Increased levels and activity
Neuroprotective
Glutamate
Neurotoxic
Ca2+
Calpain
p25
Inactive Cdk5
Active Cdk5
ROS
Increased levels and activity
Initial Stage- Neuroprotective
Glutamate
Neurotoxic
Reduced activity
Late Stage- Neurodegenerative

◀ **Fig. 8** ALDH1A1 levels and activity are independently regulated in AD clinical specimens. **a** Cdk5 kinase activity in primary cortical neurons at DIV1, DIV6, and DIV13. Cdk5 kinase assay was performed as described in the "Materials and Methods" section. Each experiment was repeated at least three independent times. *$p < 0.05$, compared with DIV1. **b** Cdk5, p35, and ALDH1A1 levels in DIV6 and DIV14 primary neurons in presence and absence of Cdk5 shRNA. The experiment was repeated two independent times, and a representative picture is presented. **c** ALDH1A1 levels in human AD and age-matched control brain tissues (cohort 1). ALDH1A1 levels were analyzed in tissues obtained from AD patients at mild ($n = 1$), moderate stage ($n = 2$), and severe stage ($n = 2$) along with age-matched controls ($n = 3$). **d** Average ALDH1A1 levels in age-matched controls and AD specimens from three independent experiments. **e** ALDH1A1 enzyme activity in age-matched controls and AD specimens from three independent experiments. **f** Same data as in Fig. 8e displaying relative ALDH1A1 activity at 90 min in age-matched controls and AD specimens from three independent experiments. **g** ALDH1A1 levels in human AD and age-matched control brain tissues (cohort 2; Table 1). **h** Average ALDH1A1 levels in age-matched controls and AD specimens from three independent experiments from cohort 2. **i** ALDH1A1 enzyme activity in age-matched controls and AD specimens from three independent experiments at 90 min from cohort 2. **j** Our model showing Cdk5's contribution to ALDH1A1-mediated signaling under physiological and pathological conditions. Under physiological conditions, Cdk5 associates with p35, which activates it resulting in upregulation of ALDH1A1, which is neuroprotective. Upon neurotoxic conditions, Cdk5 initially plays a neuroprotective role by activating and upregulating ALDH1A1. Glutamate stimulation triggers the formation of p25 formation, which hyperactivates Cdk5, leading to the phosphorylation of ALDH1A1 and subsequent increase in ALDH1A1 levels and activity. However, later, Cdk5-induced oxidative stress inhibits ALDH1A1 activity rendering it ineffective, resulting in neurotoxicity

which contained three age-matched controls, five stage II, three stage III, three stage IV, three stage V, and five stage VI specimens (details in Table 1). As observed with the previous cohort, ALDH1A1 levels increased with disease severity with highest levels observed for stage V patients (Fig. 8g). Figure 8h shows average ALDH1A1 levels in clinical specimens from three independent experiments. In addition, we also measured ALDH1A1 dehydrogenase activity in these samples, which displayed increased activity in stages II and III, which decreases as disease advances, similar to the results obtained using the previous cohort (Fig. 8i). Together, these results suggest that during the initial stages, neurons attempt to upregulate and activate ALDH1A1 to protect from ensuing oxidative stress-induced damage; however, persistently deleterious conditions inactivate ALDH1A1 in spite of increased levels, further contributing to neurotoxicity.

Discussion

An important role of ALDH1A1 in PD pathogenesis is well accepted. In normal brains, *ALDH1A1* is highly expressed in dopaminergic neurons of substantia nigra and ventral tegmental area (VTA). *ALDH1A1* level is significantly reduced in the surviving neurons of substantia nigra in PD [51]. In contrast, in schizophrenia, *ALDH1* mRNA is reduced in the VTA, but not in substantia nigra [52]. In the α-synuclein transgenic mice, both *Aldh1a1* mRNA and protein levels are decreased in dopaminergic neurons [53]. These findings highlight that loss of ALDH1 expression is correlated with selective degeneration of dopamine neurons in PD.

In contrast to PD, a role of ALDH1A1 in AD pathogenesis remains unclear. While many studies have shown that *ALDH1A1* is selectively expressed in the dopaminergic neurons, Fragoso et al. revealed that ALDH1A1 protein is also highly expressed in the human hippocampus, a region which is progressively degenerated in AD brains [54]. Although ALDH1A1 levels have not been analyzed in any clinical AD specimens, increased 4-HNE levels were indeed observed in the hippocampus of patients with mild cognitive impairment and early AD symptoms [55]. As ALDH1A1 plays crucial role in the detoxification of 4-HNE, these findings suggest that ALDH1A1 is likely inactivated or downregulated early during the disease progression. Further, 4-HNE accumulates on amyloid proteins [56], suggesting that ALDH1A1 downregulation may contribute to amyloid plaque formation at later stages of the disease as well [57, 58].

However, despite these evidence, to date, neither genome-wide association studies (GWAS) nor genetic association studies have identified any gene variation on ALDH genes as risk for AD. Furthermore, there are no reports of alterations in gene expression in any of the ALDH genes in the CNS or peripheral blood samples of AD patients compared to age-matched controls [59]. Interestingly, some reports have indicated alterations in mitochondrial ALDH2 protein in AD patients; however, ALDH1A1 protein levels or its activity has not been analyzed in AD patients.

In this study, we identified yin and yang roles of Cdk5 in the regulation of ALDH1A1. A highly destructive role of deregulated Cdk5 in AD pathogenesis is well accepted; however, our recent study revealed an initial neuroprotective role of Cdk5 in combating oxidative stress under excitotoxic conditions [42]. In this pathway, deregulated Cdk5 initially activates FOXO3a transcription factor via direct phosphorylation, which triggers its nuclear translocation, resulting in the upregulation of anti-oxidant MnSOD. However, later, active FOXO3a instead increases Bim and FasL levels, causing cell death. This finding indicates that Cdk5 might also attempt to be neuroprotective in the initial stages of neurotoxicity in AD models, but later turns neurodegenerative under sustained neurotoxic conditions.

Cdk5 exerts a multilayered regulation of ALDH1A1. ALDH1A1 is both a physiological and pathological target of Cdk5. Using primary cortical neuron maturation model, which depends on Cdk5-p35 activity, we show that Cdk5 is responsible for increase in ALDH1A1 levels under

Table 1 Details of AD specimens from cohort 2

Specimen no.	BBID no.	Autopsy no.	Age	Sex	PMI (h)	Braak stage	Neuropath Dx
1	1094	AU-16-693	100	Male	3		Control
2	915	90-A-110	81	Male	14		Control
3	1432	AU-14-1918	83	Female	21		Control
4	100	04-AA-158	87	Female	9		Control
5	508	06-AA-02	95	Female	18	2 stage II	Low-likelihood AD
6	1495	03-AA-39	89	Male	8	2 stage II	Low-likelihood AD
7	394	05-AA-196	90	Male	3	2 stage II	Intermediate-likelihood AD
8	462	10-AA-86	86	Male	21	2 stage II	Intermediate-likelihood AD
9	1181	10-AA-148	65	Female	4	2 stage II	Intermediate-likelihood AD
10	1465	10-AA-34	94	Female	9	3 stage III	Intermediate-likelihood AD
11	958	05-AA-027	82	Female	6	3 stage III	Intermediate-likelihood AD
12	1061	12-AA-172	83	Male	13	3 stage III	Intermediate-likelihood AD
13	1337	10-AA-119	89	Female	17	4 stage IV	Intermediate-likelihood AD
14	206	HI93–20432	77	Male	2	4 stage IV	Intermediate-likelihood AD
15	683	01-AA-18	68	Female	8	4 stage IV	High-likelihood AD
16	234	07-AA-50	65	Male	4	5 stage V	High-likelihood AD
17	659	10-AA-168	79	Female	Not recorded	5 stage V	High-likelihood AD
18	940	02-AA-234	91	Male	7	5 stage V	High-likelihood AD
19	1412	05-AA-171	62	Female	Not recorded	6 stage VI	High-likelihood AD
20	593	97-AA-453	65	Male	18	6 stage VI	High-likelihood AD
21	1228	99-AA-264	72	Female	9	6 stage VI	High-likelihood AD
22	352	96-AA-461	86	Female	8	6 stage VI	High-likelihood AD

physiological conditions as well (Fig. 8j, left panel). Under neurotoxic conditions, initially, Cdk5 employs three mechanisms to activate and upregulate ALDH1A1 to counteract emerging oxidative stress (Fig. 8j, middle panel). First, paradoxically, Cdk5-induced oxidative stress increases ALDH1A1 levels via transcription. Second, Cdk5 increases ALDH1A1 levels by directly phosphorylating at S75 and S274, which inhibits its ubiquitylation. Third, Cdk5-mediated phosphorylation increases its dehydrogenase activity by altering its oligomeric status. We demonstrate that ALDH1A1 is most active in the monomeric state.

Surprisingly, ALDH1A1 activity does not correlate with its levels in neuronal cells and primary neurons which uncovered the fourth mechanism by which Cdk5 negatively regulates ALDH1A1 activity. We show that the decrease in ALDH1A1 activity is due to sustained oxidative stress triggered by Cdk5 deregulation. Elimination of oxidative stress largely restored ALDH1A1 activity, thereby highlighting opposing roles of Cdk5 in the regulation of ALDH1A1 (Fig. 8j, right panel).

Importantly, under physiological conditions, Cdk5 activity is tightly regulated and is essential for normal neuronal functions. Therefore, it appears that the "good Cdk5" activates and upregulates ALDH1A1 via direct phosphorylation, without compromising its activity in normal cells. Thus, we postulate that Cdk5 plays a vital role in normal brain synaptic plasticity and memory formation by upregulating retinoic acid signaling via ALDH1A1.

The clinical significance of our finding was confirmed in human AD specimens and age-matched controls. While mild and moderate AD specimens revealed almost similar levels of ALDH1A1 as age-matched controls, the ALDH1A1 activity was significantly higher in these tissues, suggesting that the neurons upregulate ALDH1A1 activity as a compensatory mechanism to fight ensuing oxidative stress-induced damage. In contrast, severe AD brains showed significantly higher levels of ALDH1A1, but vastly compromised ALDH1A1 activity, presumably due to increased ROS. ALDH1A1 is expected to aggregate under toxic cellular conditions, which will likely inhibit its activity. Future studies are needed to uncover the dynamic equilibrium of different oligomeric forms of ALDH1A1 in clinical specimens at various stages of AD pathogenesis.

Importantly, as noted before, *ALDH1A1* levels are downregulated in the dopaminergic neurons of the substantia nigra in PD, which correlate well with neuronal death. ALDH1A1 activity was not analyzed in these tissues. However, our studies in neuronal cells, neurons, and clinical specimens revealed that ALDH1A1 protein levels and activity are independently regulated and may not necessarily correlate with each other. Higher ALDH1A1 level could be due to its aggregation in tissues, which is effectively an inactive species. Therefore, ALDH1A1 level and activity need to be independently evaluated to determine a potential role of ALDH1A1 under physiological and pathological conditions.

In conclusion, this study revealed "a good and a bad role of Cdk5" in AD pathogenesis. The bad Cdk5 prevails in the end, overriding the good Cdk5 act, suggesting that Cdk5 is an effective therapeutic target for AD. As Cdk5 is beneficial in complex with p35, and detrimental in complex with p25,

specific dissociation of Cdk5 and p25 will preserve the "good Cdk5" in the brain for retaining its physiological and beneficial functions in the brain.

Materials and Methods

Glutamate, 3-(4,5-dimethyldiazol-2-yl)-2,5-diphenyltetrazolium bromide (MTT), and poly-l-lysine were obtained from Sigma (St. Louis, MO). Roscovitine was purchased from LC Laboratories (Woburn, MA). ALDH1A1 (L-15), Cdk5 (C-8), Cdk5 (DC-17), p35 (C-19), actin (C-2), alpha-tubulin (TU-02), lamin A (H-102), and enolase (N-14) were purchased from Santa Cruz Biotech (Santa Cruz, CA) (Supplementary File 1). All antibodies were used at 1:1000 dilution. Validation for ALDH1A1 and Cdk5 antibody has been shown in Supplementary Fig. 1. HT22 cells were a gift from David Schubert. HEK293T and Phoenix cells were purchased from ATCC (Manassas, VA). HT22, HEK293T, and Phoenix cells were cultured in DMEM with 10% FBS supplemented with 2 mM glutamine and antibiotics.

Expression Plasmids and Constructs

HA-tagged ALDH1A1 was cloned into VIP3 mammalian vector and bacterial petDuet vector at EcoRI and Xho1 sites. HA-tagged ALDH1A1 mutants were generated using site-directed mutagenesis.

Expression and Purification of Cdk5, p25, and ALDH1A1

6× His-Cdk5 and 6× His-p25 were prepared using the baculovirus Bac-to-Bac expression system according to the manufacturer's instructions (Invitrogen). 6× His-tagged wild-type and mutant ALDH1A1 were expressed in *E. coli* and purified using the procedures previously described [38].

Transfection and Retroviral Infection

For generating stable cell lines, ALDH1A1 plasmids were transiently transfected using calcium phosphate into Phoenix cells. The retroviruses were harvested and used to infect HT22 cells as reported previously [31, 32].

In Vitro Kinase Assays

For in vitro labeling, Cdk5-p25 complex (on Ni-NTA beads) was pre-incubated with 100 μM of ATP for 1 h in a 1× kinase buffer (50 mM Tris, 10 mM $MgCl_2$) to reduce background phosphorylation. The beads were washed extensively with 1× kinase buffer to remove excess ATP, eluted, and then subjected to an in vitro kinase assay with 2 μg of 6× His-tagged recombinant protein (wild-type or mutant ALDH1A1) in the presence of 0.5 μCi of [γ-^{32}P]ATP for 15 min. Reactions were terminated upon the addition of SDS loading buffer and subsequently separated by SDS-PAGE gel, transferred to PVDF membrane, and exposed for autoradiography.

ALDH1A1 shRNA

Cdk5 shRNAs were generated in our previous study [40]. Both Cdk5 and ALDH1A1 shRNAs (both were murine as HT22 cells are mouse hippocampal cells) were cloned into pLKO.1 TRC vector, which was a gift from David Root [60]. The sequences are as follows: *ALDH1A1 shRNA1* (forward) 5′-C CGG ATC TCA TTG AGA GTG GGA AGA CTC GAG TCT TCC CAC TCT CAA TGA GAT TTT TTG-3′, *ALDH1A1 shRNA1* (reverse) 5′-A ATT CAA AAA ATC TCA TTG AGA GTG GGA AGA CTC GAG TCT TCC CAC TCT CAA TGA GAT-3′ and *ALDH1A1 shRNA2* (forward) 5′-C CGG GCA GGA CTC TTC ACT AAA CTC GAG TTT AGT GAA GAG TCC TGC TTT TTG-3′, *ALDH1A1 shRNA2* (reverse) 5′-A ATT CAA AAA GCA GGA CTC TTC ACT AAA CTC GAG TTT AGT GAA GAG TCC TGC-3′. Control shRNA (scrambled shRNA), Cdk5, and ALDH1A1 shRNA lentiviruses were generated and used for infecting HT22 cells. Stable cells were generated following puromycin selection.

Isolation of Primary Cortical Neurons

The primary cortical neurons were isolated from E17 CD1 mice embryos as reported before [40, 41]. All the experiments were performed after 14 days in culture, except otherwise mentioned.

MTT Assay

Cells were seeded in 96-well plates at 5×10^3 cells per 100 μL per well and cultured for 24, 48, and 72 h. MTT assay was conducted as reported previously [43]. Experiments were repeated three times in triplicate wells to ensure the reproducibility.

Immunofluorescence

HT22 cells were grown on poly-L-lysine coated coverslips for 12 h, followed by various treatments. Roscovitine (10 μM) was added 0.5 h before glutamate treatment, and Cdk5 shRNA lentivirus was added 30 h prior to glutamate treatment. Cells were fixed with 4% formaldehyde in PBS for 20 min at room temperature, and then washed with PBS. The cells were blocked in 1% FBS, 2% BSA, and 0.1% Triton X-100 in PBS for 1 h at 25 °C. Cells were labeled with antibodies (Cdk5 or ALDH1A1 or HA) for 3 h in PBS, followed by incubation with fluorescein isothiocyanate conjugated goat anti-mouse-IgG secondary antibody (1:1000 dilution, cat. no. 115–095-003, Jackson Immunoresearch), fluorescein isothiocyanateconjugated donkey anti-rabbit-IgG secondary antibody (1:1000 dilution, cat. no. 711–095-152, Jackson Immunoresearch), Texas Red-conjugated goat anti-rabbit-IgG secondary antibody (1:500 dilution, T6391, Invitrogen), or Texas Red-conjugated goat anti-mouse-IgG secondary antibody (1:500 dilution, cat. no. T6390, Invitrogen). Cells were visualized using Nikon Eclipse E600 microscope (Nikon Instruments, Melville, NY) and captured. To quantify cytoplasmic and nuclear localization, the average fluorescence intensity in the nucleus was compared with the average fluorescence intensity in the cytosol. This value was plotted for different treatment times with respect to untreated cells.

Immunoprecipitation of Cdk5, p35/p25, and ALDH1A1

HT22 cells were treated with 5 mM glutamate for 1.5, 3, or 6 h. Cells were then harvested and lysed in modified RIPA buffer. After centrifugation, whole-cell lysate was mixed with protein A Sepharose beads (Sigma) and antibody for either Cdk5, p35/p25, or ALDH1A1. After incubation for 4 h, immune complexes were washed and then subjected to Western blotting using either Cdk5, p35/p25, or ALDH1A1 antibodies.

Subcellular Fractionation

Subcellular fractionation of HT22 cells was conducted as before [40].

ALDH1A1 Activity Assay

ALDH1A1 activity assay was conducted as reported before [36]. Briefly, ALDH1A1 was phosphorylated using Cdk5-p25 in kinase buffer (37.5 mM HEPES pH 8.00, 300 μM ATP, 4 mM $MgCl_2$) for 3 h. Subsequently, the reaction mixture was adjusted to contain 100 mM HEPES pH 8.00, 77.4 μM ATP, 1 mM $MgCl_2$, 0.65% BSA, 5 mM NAD^+, and 4 mM propanal. The change in absorbance at 360 nm due to NADH formation was measured using SpectraFluor PLUS, TECAN. The data is shown as the fractional conversion of NAD^+ to NADH to highlight the relative intrinsic activity of the wild-type and mutant ALDH1A1 and effect of Cdk5-dependent phosphorylation. For dephosphorylation experiment, phosphorylated ALDH1A1 activity was measured for 75 min, at which time 1 μL of calf-alkaline phosphatase was added to the sample and the measurements were carried out for another 1.5 h. For untreated samples, 50% glycerol in 1× cutsmart buffer (New England Biolab) was added as a control.

Native Gel Analysis of Cdk5-p25 Mediated ALDH1A1 Phospho-Oligomeric Regulation

6× His-Cdk5-p25 on beads was used to phosphorylate ALDH1A1 (~0.5 mg/mL) in kinase buffer containing 50 mM Tris pH 8.00, 10 mM $MgCl_2$ 50 mM NaCl, 50 mM imidazole, and 1 mM ATP. Importantly, when high concentrations of ALDH1A1 were used (> 1 mg/mL), the change from tetramer to monomer was less pronounced. For the first time point, the reaction was spun down and 10 μL of the supernatant was mixed with 5 μL of 3× native running buffer containing 10 mM EDTA to stop the kinase reaction. The reaction tube was subsequently placed on a thermomixer (800 rpm) at room temperature. Ten-microliter aliquots of the supernatant were collected at each time point indicated. The samples were separated using clear-native PAGE (CN-PAGE) with a 7.5% resolving gel (pH 8.9) and a 4.3% stacking gel (pH 6.7). Following electrophoresis, the gel was soaked in 1× SDS page running buffer for 5 min to denature complexes, followed by 1× transfer buffer containing 20% methanol to remove excess SDS. Proteins were transferred and ALDH1A1 was visualized using ALDH1A1 antibody. All experiments were performed three independent times in triplicate.

In-Gel ALDH1A1 Activity Assay

In-gel ALDH1A1 activity was determined as reported before [36].

Oligomer-Specific Phosphorylation of ALDH1A1

ALDH1A1 was phosphorylated using Cdk5-p25 for 0, 10, and 30 min. Following CN-PAGE, the gels were fixed in 10% acetic acid and 30% methanol for 20 min and washed 3× for 5 min with water. Phospho-tag phosphoprotein gel staining was carried out according to the manufacturer's protocol (Genecopoeia). Gels were imaged using a Typhoon© scanner equipped with a phospho-tag filter. Following fluorescent detection, total protein levels were visualized with Coomassie G-250 staining. All experiments were carried out in triplicate.

Semi-Quantitative PCR

Total RNA were extracted from control and treated cells using Trizol reagent (Invitrogen). Samples were quantified and transcribed using the RT-PCR Kit (Promega) according to manufacturer's instructions. Primers for ALDH1A1 and β-actin were designed and standardized in the laboratory. The primer sequences for ALDH1A1 were as follows: 5-GGA AAT GGA AGA GAA CTG GGT GA-3 (sense) and 5-GAG CTT GCG CTT ATA TCT ATC CTT C-3 (anti-sense). For β-actin, the primer sequences were 5-CAT GTA CGT TGC TAT CCA GGC-3 (sense) and 5-CTC CTT AAT GTC ACG CAC GAT-3 (anti-sense). PCR conditions were optimized to maintain amplification in the linear range to avoid the plateau effect. PCR products were then separated on a 2% agarose gel, visualized in a gel documentation system, and photographed. Band intensity on gels was analyzed using ImageJ 1.43 software (NIH, Bethesda, MD) and normalized to β-actin PCR products. Each RT-PCR experiment was repeated three independent times.

Real-Time qPCR

To determine the change in expression of the ALDH1A1 genes, real-time qPCR was performed. Total RNA were extracted from control and treated cells using Trizol reagent (Invitrogen). Samples were quantified and transcribed using the RT-PCR Kit (Promega) according to manufacturer's instructions. ALDH1A1 forward primer 5′-AGA GGA GAT ATT TGG ACC AGT GC-3′ and reverse primer 5′-GGC TGA CAA CAT CAT ATA GCA GT-3′ and β-actin forward 5′-CAT GTA CGT TGC TAT CCA GGC-3′ and reverse primer 5′-CTC CTT AAT GTC ACG CAC GAT-3′ were designed and standardized in the laboratory. All the reactions were performed in triplicate and SYBR Green Supermix (Bio-Rad) was used as fluorescent dye in Biorad CFX Connect™. Thermal cycling was initiated at 94 °C for 4 min, followed by 35 cycles of PCR (94 °C, 15 s; 51 °C, 30 s; 72 °C, 30 s). β-Actin was used as an endogenous control, and vehicle control was used as a calibrator. The relative changes in gene expression were calculated using the following formula: fold change in gene expression, $2 - \Delta\Delta Ct = 2 - \{\Delta Ct$ (treated samples) $- \Delta Ct$ (untreated control samples)$\}$, where $\Delta Ct = Ct$ (genes of interest) $- Ct$ (β-actin) and Ct represents the threshold cycle number.

Ubiquitylation Assay

HT22, ALDH1A1-HT22, and 2A-ALDH1A1-HT22 cells were transfected with 6× His ubiquitin, followed by glutamate treatment for 12 h in the presence and absence of roscovitine or Cdk5 shRNA. After 6 h of glutamate treatment, MG132 (Sigma-Aldrich) was added to a final concentration of 10 μM for an additional 6 h to stabilize ubiquitylated proteins. After 12 h of glutamate treatment, cells were lysed and ALDH1A1–1 was immunoprecipitated using anti-ALDH1A1/HA antibody. The proteins were then separated by SDS-PAGE, and potential ubiquitylation was analyzed using anti-6× His antibody. Each experiment was performed at least three times independently.

Statistical Analysis

Data are expressed as mean ± SEM and were statistically evaluated with one-way ANOVA, followed by the Bonferroni post hoc test using GraphPad Prism 5.04 software (GraphPad Software). $P < 0.05$ was considered statistically significant.

Acknowledgements This work was supported by the National Institute on Aging (R21-AG 47447 to KS.). We thank Dr. David Schubert for the HT22 cells. pLKO.1 TRC vector was a gift from David Root (Addgene plasmid #10878) [60]. We thank New York Brain Bank for the cohort 1 clinical specimens (NIH P50 AG008702) and Michigan Brain Bank (University of Michigan Alzheimer's Disease Core Center supported by 5P30 AG053760) for providing the cohort 2 clinical specimens (Table 1).

Authors' Contributions KN conducted all experiments except in vitro kinase assays. KV performed in vitro kinase assays (Figs. 1a and 3a, b). KS analyzed the data and wrote the manuscript. All authors read and approved the final manuscript.

Funding This work was supported by grant from National Institute on Aging, National Institutes of Health (R21-AG 47447).

Compliance with Ethical Standards

Competing Interests The authors declare that they have no competing interests.

References

1. Castellani RJ, Perry G (2014) The complexities of the pathology-pathogenesis relationship in Alzheimer disease. Biochem Pharmacol 88(4):671–676. https://doi.org/10.1016/j.bcp.2014.01.009
2. Lane MA, Bailey SJ (2005) Role of retinoid signalling in the adult brain. Prog Neurobiol 75(4):275–293. https://doi.org/10.1016/j.pneurobio.2005.03.002
3. Goncalves MB, Clarke E, Hobbs C, Malmqvist T, Deacon R, Jack J, Corcoran JP (2013) Amyloid β inhibits retinoic acid synthesis exacerbating Alzheimer disease pathology which can be attenuated by an retinoic acid receptor α agonist. Eur J Neurosci 37(7):1182–1192. https://doi.org/10.1111/ejn.12142
4. Kawahara K, Suenobu M, Ohtsuka H, Kuniyasu A, Sugimoto Y, Nakagomi M, Fukasawa H, Shudo K et al (2014) Cooperative therapeutic action of retinoic acid receptor and retinoid x receptor agonists in a mouse model of Alzheimer's disease. J Alzheimers Dis 42(2):587–605. https://doi.org/10.3233/JAD-132720.
5. Wang X, Tan L, Lu Y, Peng J, Zhu Y, Zhang Y, Sun Z (2015) MicroRNA-138 promotes tau phosphorylation by targeting retinoic

acid receptor alpha. FEBS Lett 589(6):726–729. https://doi.org/10.1016/j.febslet.2015.02.001
6. Cheung ZH, Ip NY (2015) Cdk5: A multifaceted kinase in neurodegenerative diseases. Mini Rev Med Chem 15(5):390–395. https://doi.org/10.1016/j.tcb.2011.11.003
7. Shukla V, Skuntz S, Pant HC (2012) Deregulated Cdk5 activity is involved in inducing Alzheimer's disease. Arch Med Res 43(8):655–662. https://doi.org/10.1016/j.arcmed.2012.10.015
8. Shah K, Lahiri DK (2014) Cdk5 activity in the brain - multiple paths of regulation. J Cell Sci 127(11):2391–2400. https://doi.org/10.1242/jcs.147553
9. Shah K, Lahiri DK (2017) A tale of the good and bad: Remodeling of the microtubule network in the brain by Cdk5. Mol Neurobiol 54(3):2255–2268. https://doi.org/10.1007/s12035-016-9792-7
10. Shah K, Rossie S (2018) Tale of the good and bad Cdk5: Remodeling of the actin cytoskeleton in the brain. Mol Neurobiol 55:3426–3438. https://doi.org/10.1007/s12035-017-0525-3
11. Sun KH, Chang KH, Clawson S, Ghosh S, Mirzaei H, Regnier F, Shah K (2011) Glutathione S-transferase P1 is a critical regulator of Cdk5 kinase activity. J Neurochem 118(5):902–914. https://doi.org/10.1111/j.1471-4159.2011.07343.x
12. Ohshima T, Ward JM, Huh CG, Longenecker G, Veeranna, Pant HC, Brady RO, Martin LJ, Kulkarni AB. (1996) Targeted disruption of the cyclin-dependent kinase 5 gene results in abnormal corticogenesis, neuronal pathology and perinatal death. Proc Natl Acad Sci U S A 93(20):11173–11178.
13. Heller EA, Hamilton PJ, Burek DD, Lombroso SI, Peña CJ, Neve RL, Nestler EJ (2016) Targeted epigenetic remodeling of the Cdk5 gene in nucleus Accumbens regulates cocaine- and stress-evoked behavior. J Neurosci 36(17):4690–4697. https://doi.org/10.1523/JNEUROSCI.0013-16.2016
14. Hernandez A, Tan C, Mettlach G, Pozo K, Plattner F, Bibb JA (2016) Cdk5 modulates long-term synaptic plasticity and motor learning in dorsolateral striatum. Sci Rep 6:29812. https://doi.org/10.1038/srep29812
15. Venturin M, Guarnieri P, Natacci F, Stabile M, Tenconi R, Clementi M., Hernandez C, Thompson, P, Upadhyaya M, Larizza L, Riva P. (2004) Mental retardation and cardiovascular malformations in NF1 microdeleted patients point to candidate genes in 17q11.2. J Med Genet 41:35–41.
16. Engmann O, Hortobágyi T, Pidsley R, Troakes C, Bernstein HG, Kreutz MR, Mill J, Nikolic, M., Giese, K.P. (2011) Schizophrenia is associated with dysregulation of a Cdk5 activator that regulates synaptic protein expression and cognition. Brain 134(8):2408–2421. doi: https://doi.org/10.1093/brain/awr155.
17. Patel LS, Wenzel HJ, Schwartzkroin PA (2004) Physiological and morphological characterization of dentate granule cells in the p35 knock-out mouse hippocampus: Evidence for an epileptic circuit. J Neurosci 24(41):9005–9014. https://doi.org/10.1523/JNEUROSCI.2943-04.2004
18. Drerup JM, Hayashi K, Cui H, Mettlach GL, Long MA, Marvin M, Sun X, Goldberg MS et al (2010) Attention-deficit/hyperactivity phenotype in mice lacking the cyclin-dependent kinase 5 cofactor p35. Biol Psychiatry 68(12):1163–1171. https://doi.org/10.1016/j.biopsych.2010.07.016
19. Hisanaga S, Endo R (2010) Regulation and role of cyclin-dependent kinase activity in neuronal survival and death. J Neurochem 115(6):1309–1321. https://doi.org/10.1111/j.1471-4159.2010.07050.x
20. Meyer DA, Torres-Altoro MI, Tan Z, Tozzi A, Di Filippo M, DiNapoli V, Plattner F, Kansy JW et al (2014) Ischemic stroke injury is mediated by aberrant Cdk5. J Neurosci 34(24):8259–8267. https://doi.org/10.1523/JNEUROSCI.4368-13.2014
21. Sun KH, Lee HG, Smith MA, Shah K (2009) Direct and indirect roles of cyclin-dependent kinase 5 as an upstream regulator in the c-Jun NH2-terminal kinase cascade: Relevance to neurotoxic insults in Alzheimer's disease. Mol Biol Cell 20(21):4611–4619. https://doi.org/10.1091/mbc.E09-05-0433
22. Chang KH, Pablo Y, Lee H, Lee H, Smith MA, Shah K (2010) Cdk5 is a major regulator of p38 Cascade: Relevance to neurotoxicity in Alzheimer's disease. J Neurochem 113(5):1221–1229. https://doi.org/10.1111/j.1471-4159.2010.06687.x.
23. Shukla V, Seo J, Binukumar BK, Amin ND, Reddy P, Grant P, Kuntz S, Kesavapany S et al (2017) TFP5, a peptide inhibitor of aberrant and hyperactive Cdk5/p25, attenuates pathological phenotypes and restores synaptic function in CK-p25Tg mice. J Alzheimers Dis 56(1):335–349. https://doi.org/10.3233/JAD-160916
24. Jackson B, Brocker C, Thompson DC, Black W, Vasiliou K, Nebert DW, Vasiliou V (2011) Update on the aldehyde dehydrogenase gene (ALDH) superfamily. Hum Genomics 5(4):283–303
25. Singh S, Brocker C, Koppaka V, Chen Y, Jackson BC, Matsumoto A, Thompson DC, Vasiliou V (2013) Aldehyde dehydrogenases in cellular responses to oxidative/electrophilic stress. Free Radic Biol Med 56:89–101. https://doi.org/10.1016/j.freeradbiomed.2012.11.010
26. Grünblatt E, Riederer P. (2016) Aldehyde dehydrogenase (ALDH) in Alzheimer's and Parkinson's disease. J Neural Transm (Vienna). (2):83–90. doi: https://doi.org/10.1007/s00702-014-1320-1.
27. Zhang M, Shoeb M, Goswamy J, Liu P, Xiao TL, Hogan D, Campbell GA, Ansari NH (2010) Overexpression of aldehyde dehydrogenase1A1 reduces oxidation-induced toxicity in SH-SY5Y neuroblastoma cells. J Neurosci Res 88(3):686–694. https://doi.org/10.1002/jnr.22230.
28. Kong D, Kotraiah V (2012) Modulation of aldehyde dehydrogenase activity affects (±)-4-hydroxy-2E-nonenal (HNE) toxicity and HNE-protein adduct levels in PC12 cells. J Mol Neurosci 47(3):595–603. https://doi.org/10.1007/s12031-011-9688-y
29. Yuan XZ, Sun S, Tan CC, Yu JT, Tan L (2017) The role of ADAM10 in Alzheimer's disease. J Alzheimers Dis 58(2):303–322. https://doi.org/10.3233/JAD-170061
30. Shah K, Liu Y, Deirmengian C, Shokat KM (1997) Engineering unnatural nucleotide specificity for Rous sarcoma virus tyrosine kinase to uniquely label its direct substrates. Proc Natl Acad Sci U S A 94:3565–3570
31. Shah K, Shokat KM (2002) A chemical genetic screen for direct v-Src substrates reveals ordered assembly of a retrograde signaling pathway. Chem Biol 9(1):35–47
32. Shah K, Vincent F (2005) Divergent roles of c-Src in controlling platelet-derived growth factor-dependent signaling in fibroblasts. Mol Biol Cell 16(11):5418–5432. https://doi.org/10.1091/mbc.E05-03-0263
33. Kim S, Shah K (2007) Dissecting yeast Hog1 MAP kinase pathway using a chemical genetic approach. FEBS Lett 581(6):1209–1216. https://doi.org/10.1016/j.febslet.2007.02.032
34. Johnson EO, Chang KH, de Pablo Y, Ghosh S, Mehta R, Badve S, Shah K (2011) PHLDA1 is a crucial negative regulator and effector of aurora a kinase in breast Cancer. J Cell Sci 124(16):2711–2722. https://doi.org/10.1242/jcs.084970
35. Johnson EO, Chang KH, Ghosh S, Venkatesh C, Giger K, Low PS, Shah K (2012) LIMK2 is a crucial regulator and effector of aurora-A-kinase-mediated malignancy. J Cell Sci 125(5):1204–1216. https://doi.org/10.1242/jcs.092304
36. Wang J, Nikhil K, Viccaro K, Lei C, White J, Shah K (2017) Phosphorylation-dependent regulation of ALDH1A1 by aurora kinase a: Insights on their synergistic relationship in pancreatic Cancer. BMC Biol 15(1):1–10. https://doi.org/10.1186/s12915-016-0335-5.
37. Wang J, Nikhil K, Viccaro K, Lei C, Jacobsen M, Sandusky G, Shah K (2017) Aurora A-Twist1 Axis promotes highly aggressive phenotypes in pancreatic carcinoma. J Cell Sci 130(6):1078–1093. https://doi.org/10.1242/jcs.196790.

38. Sun KH, de Pablo Y, Vincent F, Johnson EO, Chavers AK, Shah K (2008) Novel genetic tools reveal Cdk5's major role in Golgi fragmentation in Alzheimer's disease. Mol Biol Cell 19(7):3052–3069. https://doi.org/10.1091/mbc.E07-11-1106
39. Sun KH, de Pablo Y, Vincent F, Shah K (2008) Deregulated Cdk5 promotes oxidative stress and mitochondrial dysfunction. J Neurochem 107(1):265–278. https://doi.org/10.1111/j.1471-4159.2008.05616.x
40. Chang KH, Multani PS, Sun KH, Vincent F, de Pablo Y, Ghosh S, Gupta R, Lee HP et al (2011) Nuclear envelope dispersion triggered by deregulated Cdk5 precedes neuronal death. Mol Biol Cell 22(9):1452–1462. https://doi.org/10.1091/mbc.E10-07-0654
41. Chang KH, Vincent F, Shah K (2012) Deregulated Cdk5 triggers aberrant activation of cell cycle kinases and phosphatases inducing neuronal death. J Cell Sci 125(21):5124–5137. https://doi.org/10.1242/jcs.108183
42. Shi C, Viccaro K, Lee HG, Shah K (2016) Cdk5-FOXO3a axis: Initially neuroprotective, eventually neurodegenerative in Alzheimer's disease models. J Cell Sci 129:1815–1830. https://doi.org/10.1242/jcs.185009
43. Nikhil K, Shah K (2017) Cdk5-Mcl-1 Axis promotes mitochondrial dysfunction and neurodegeneration in Alzheimer disease model. J Cell Sci 130(18):3023–3039. https://doi.org/10.1242/jcs.205666.
44. Marchitti SA, Brocker C, Stagos D, Vasiliou V (2008) Non-P450 aldehyde oxidizing enzymes: The aldehyde dehydrogenase superfamily. Expert Opin Drug Metab Toxicol 4(6):697–720. https://doi.org/10.1517/17425255.4.6.697
45. Ayala A, Muñoz MF, Argüelles S. (2014) Lipid peroxidation: production, metabolism, and signaling mechanisms of malondialdehyde and 4-hydroxy-2-nonenal. Oxid Med Cell Longev. 360438. doi: https://doi.org/10.1155/2014/360438.
46. Tan S, Sagara Y, Liu Y, Maher P, Schubert D (1998) The regulation of reactive oxygen species production during programmed cell death. J Cell Biol 141:1423–1432
47. Hosie KA, King AE, Blizzard CA, Vickers JC, Dickson TC. (2012) Chronic excitotoxin-induced axon degeneration in a compartmented neuronal culture model. ASN Neuro. 4(1):pii: e00076. doi: https://doi.org/10.1042/AN20110031.
48. Nikolic M, Dudek H, Kwon YT, Ramos YF, Tsai LH (1996) The cdk5/p35 kinase is essential for neurite outgrowth during neuronal differentiation. Genes Dev 10(7):816–825
49. Braak H, Braak E (1991) Neuropathological staging of Alzheimer-related changes. Acta Neuropathol 82(4):239–259
50. Bussière T, Giannakopoulos P, Bouras C, Perl DP, Morrison JH, Hof PR (2003) Progressive degeneration of nonphosphorylated neurofilament protein-enriched pyramidal neurons predicts cognitive impairment in Alzheimer's disease: Stereologic analysis of prefrontal cortex area 9. J Comp Neurol 463:281–302. https://doi.org/10.1002/cne.10760
51. Mandel S, Grunblatt E, Riederer P, Amariglio N, Jacob-Hirsch J, Rechavi G, Youdim MB (2005) Gene expression profiling of sporadic Parkinson's disease substantia nigra pars compacta reveals impairment of ubiquitin-proteasome subunits, SKP1A, aldehyde dehydrogenase, and chaperone HSC-70. Ann N Y Acad Sci 1053:356–375. https://doi.org/10.1196/annals.1344.031
52. Galter D, Buervenich S, Carmine A, Anvret M, Olson L (2003) ALDH1 mRNA: Presence in human dopamine neurons and decreases in substantia nigra in Parkinson's disease and in the ventral tegmental area in schizophrenia. Neurobiol Dis 14(3):637–647
53. Liu G, Yu J, Ding J, Xie C, Sun L, Rudenko I, Zheng W, Sastry N et al (2014) Aldehyde dehydrogenase 1 defines and protects a nigrostriatal dopaminergic neuron subpopulation. J Clin Invest 124(7):3032–3046. https://doi.org/10.1172/JCI72176
54. Fragoso YD, Shearer KD, Sementilli A, de Carvalho LV, McCaffery PJ (2012) High expression of retinoic acid receptors and synthetic enzymes in the human hippocampus. Brain Struct Funct 217(2):473–483. https://doi.org/10.1007/s00429-011-0359-0
55. Williams TI, Lynn BC, Markesbery WR, Lovell MA (2006) Increased levels of 4-hydroxynonenal and acrolein, neurotoxic markers of lipid peroxidation, in the brain in mild cognitive impairment and early Alzheimer's disease. Neurobiol Aging 27:1094–1099. https://doi.org/10.1016/j.neurobiolaging.2005.06.004
56. Sayre LM, Zelasko DA, Harris PL, Perry G, Salomon RG, Smith MA (1997) 4-Hydroxynonenal-derived advanced lipid peroxidation end products are increased in Alzheimer's disease. J Neurochem 68:2092–2097
57. Ando Y, Brannstrom T, Uchida K, Nyhlin N, Nasman B, Suhr O, Yamashita T, Olsson T et al (1998) Histochemical detection of 4-hydroxynonenal protein in Alzheimer amyloid. J Neurol Sci 156:172–176
58. McGrath LT, McGleenon BM, Brennan S, McColl D, Mc IS, Passmore AP (2001) Increased oxidative stress in Alzheimer's disease as assessed with 4-hydroxynonenal but not malondialdehyde. QJM 94:485–490
59. Maes OC, Schipper HM, Chertkow HM, Wang E (2009) Methodology for discovery of Alzheimer's disease blood-based biomarkers. J Gerontol A Biol Sci Med Sci 64(6):636–645. https://doi.org/10.1093/gerona/glp045.
60. Moffat J, Grueneberg DA, Yang X, Kim SY, Kloepfer AM, Hinkle G, Piqani B, Eisenhaure TM et al (2006) A lentiviral RNAi library for human and mouse genes applied to an arrayed viral high-content screen. Cell 124(6):1283–1298. https://doi.org/10.1016/j.cell.2006.01.040